



Stable isotope ($\delta^{13}\text{C}$, $\delta^{18}\text{O}$) paleoecology of the late Early Miocene mammalian fauna from Buluk, Kenya

Irisa D. Arney, Ellis M. Locke, Ellen R. Miller, and Isaiah O. Nengo

ABSTRACT

Early Miocene deposits at Buluk in northern Kenya have produced an abundant and diverse community of mammalian fossils, including catarrhine primates, and the site is an important resource for characterizing habitat heterogeneity across East Africa during the early-middle Miocene transition. Here we present the results of stable carbon and oxygen isotope analyses of fossil tooth enamel from Buluk's ruminant artiodactyls, suids, anthracotheres, rhinocerotids, proboscideans, and hyraxes, to address the nature of the C₃ vegetation (i.e., open-canopy versus closed-canopy and/or degree of water stress) and to determine whether C₄ plants were a dietary component of Buluk herbivores. $\delta^{13}\text{C}_{\text{enamel}}$ and $\delta^{18}\text{O}_{\text{enamel}}$ values indicate that most Buluk herbivores foraged in a C₃-dominated mosaic of open canopy woodland habitats with no evidence of closed-canopy habitats, consistent with soil and biomarker analyses. Despite paleosol evidence for the presence of C₄ vegetation at Buluk, $\delta^{13}\text{C}_{\text{enamel}}$ results show no evidence for the consumption of C₄ biomass. This discrepancy may be caused by the presence of C₄ vegetation on the landscape that was not consumed by local herbivores in quantities that can be captured by bulk $\delta^{13}\text{C}_{\text{enamel}}$, lack of sampling of taxa that did consume C₄ vegetation, or it may reflect differences in scale between these two data sources. Overall, the range of $\delta^{13}\text{C}_{\text{enamel}}$ values from Buluk are like the early Miocene site of Moroto and are significantly more enriched than the middle Miocene localities Maboko Island and Fort Ternan, suggesting more water-stressed environments predominated at these earlier Miocene sites in East Africa.

Irisa D. Arney. Western University of Health Sciences, College of Osteopathic Medicine of the Pacific Northwest, Lebanon, Oregon 97355, USA. (corresponding author) iarney@westernu.edu

Ellis M. Locke. Idaho College of Osteopathic Medicine, Meridian, Idaho 83642, USA. elocke@icom.edu

Ellen R. Miller. Wake Forest University, Department of Anthropology, Winston Salem, North Carolina 27109, USA. millerer@wfu.edu

Isaiah O. Nengo, deceased. Formerly of Turkana Basin Institute, Social and Behavioral Sciences, Stony Brook University, Stony Brook, New York 11794, USA.

Final citation: Arney, Irisa D., Locke, Ellis M., Miller, Ellen R., and Nengo, Isaiah O. 2024. Stable isotope ($\delta^{13}\text{C}$, $\delta^{18}\text{O}$) paleoecology of the late Early Miocene mammalian fauna from Buluk, Kenya. *Palaeontologia Electronica*, 27(1):a19.

<https://doi.org/10.26879/1335>

palaeo-electronica.org/content/2024/5121-buluk-kenya-stable-isotopes

Copyright: March 2024 Society of Vertebrate Paleontology.

This is an open access article distributed under the terms of the Creative Commons Attribution License, which permits unrestricted use, distribution, and reproduction in any medium, provided the original author and source are credited.

creativecommons.org/licenses/by/4.0/

Key Words: carbon isotopes; East Africa; Miocene; paleoenvironment; herbivores; C₃ diets

Submission: 31 August 2023. Acceptance: 10 January 2024.

INTRODUCTION

Buluk is the easternmost early Miocene primate locality in Africa, and as such the site is a meaningful point of comparison for documenting both spatial and temporal heterogeneity of East African habitats across the early-middle Miocene transition. A growing body of paleoenvironmental evidence suggests that the early Miocene of East Africa was characterized by substantial spatial and temporal variation in climatic conditions and vegetation (Retallack et al., 2002; Bonnefille, 2010; Michel et al., 2014, 2020; Lukens et al., 2017a, 2021; Butts, 2019; Liutkus-Pierce et al., 2019; Baumgartner and Peppe, 2021; Peppe et al., 2023). While forests are documented at some early Miocene sites in western Kenya (e.g., Michel et al., 2014, 2020; Oginga, 2018; Baumgartner and Peppe, 2021), open woodland and wooded grassland environments are also well documented both in western Kenya (Driese et al., 2016; Lukens et al., 2017a) and northern Kenya (Lukens et al., 2017b, 2021; Butts, 2019; Liutkus-Pierce et al., 2019).

Soil and plant wax geochemical and palaeobotanical evidence for some contribution of C₄ vegetation to open woodland habitats has been recovered at several early Miocene localities in East Africa, including at Buluk (Lukens et al., 2017a, 2021; Peppe et al., 2023). Whether early Miocene herbivorous mammals had begun to incorporate these C₄ resources into their diets is less clear. Dental morphological data suggest that grazing adaptations were not present among ruminants until the late Miocene (Hall and Cote, 2021), and published information about herbivore enamel isotopic evidence prior to 10 Ma is largely lacking (Cerling et al., 1997; Arney et al., 2022; MacLatchy et al., 2023). Buluk's mammalian assemblage provides an opportunity to add to the regional record of habitat variation in the early Miocene of East Africa and to retrodict the dietary behavior of herbivores that inhabited these environments. To this end, we report the results of enamel stable isotope analyses ($\delta^{13}\text{C}_{\text{enamel}}$; $\delta^{18}\text{O}_{\text{enamel}}$) from a range of fossil mammalian herbivores at Buluk with two objectives: 1) to establish dietary isotopic ranges for fossil herbivore guilds; and 2) to examine inter-

site variation in $\delta^{13}\text{C}_{\text{enamel}}$ values to assess niche partitioning among early and middle Miocene herbivores.

Toward the first objective, we establish carbon isotopic profiles for the major mammalian herbivore groups from Buluk to examine dietary niche partitioning at the site and to determine whether C₄ vegetation was a dietary component for any of the sampled groups. Several past $\delta^{13}\text{C}_{\text{enamel}}$ studies exploring the vegetation history of East Africa during the Neogene found that landscapes in the early and middle Miocene were C₃-dominated with little to no C₄ biomass (Cerling et al., 1991, 1997; Uno et al., 2011, 2016; Feakins et al., 2013; Polissar et al., 2019). This paradigm was recently challenged by the recovery of geochemical evidence from plant wax and soil carbonates, which indicated heterogeneous environments including C₄ grasses were present at multiple early Miocene localities (Peppe et al., 2023). $\delta^{13}\text{C}_{\text{enamel}}$ values from herbivorous mammals at Buluk will allow us to assess whether C₄ grasses or water-stressed C₃ vegetation were being ingested by these animals. In addition, $\delta^{18}\text{O}$ values are used to characterize the drinking habits utilized by mammalian herbivores, and to assess the implications for local environmental aridity at Buluk.

The second objective is to compare Buluk $\delta^{13}\text{C}_{\text{enamel}}$ values with those from published records of two Middle Miocene localities in Western Kenya: Maboko Island (~15-14 Ma; Feibel and Brown, 1991) and Fort Ternan (13.7 Ma; Pickford et al., 2006), and the Ugandan Early Miocene locality Moroto (21 Ma; MacLatchy et al., 2023) to examine inter-site variation among common taxa. Inferred open habitats at Maboko (Evans et al., 1981; Retallack et al., 2002; Arney et al., 2022) and Fort Ternan (Evans et al., 1981; Shipman et al., 1981; Shipman, 1986; Retallack et al., 1990; Kappelman, 1991; Retallack, 1992; Cerling et al., 1991, 1997; Dugas and Retallack, 1993) have played a key role in framing the early-middle Miocene ecological transition. Additionally, Moroto, Maboko, and Fort Ternan are the only East African localities with $\delta^{13}\text{C}_{\text{enamel}}$ values that provide comparative values for interpreting niche partitioning

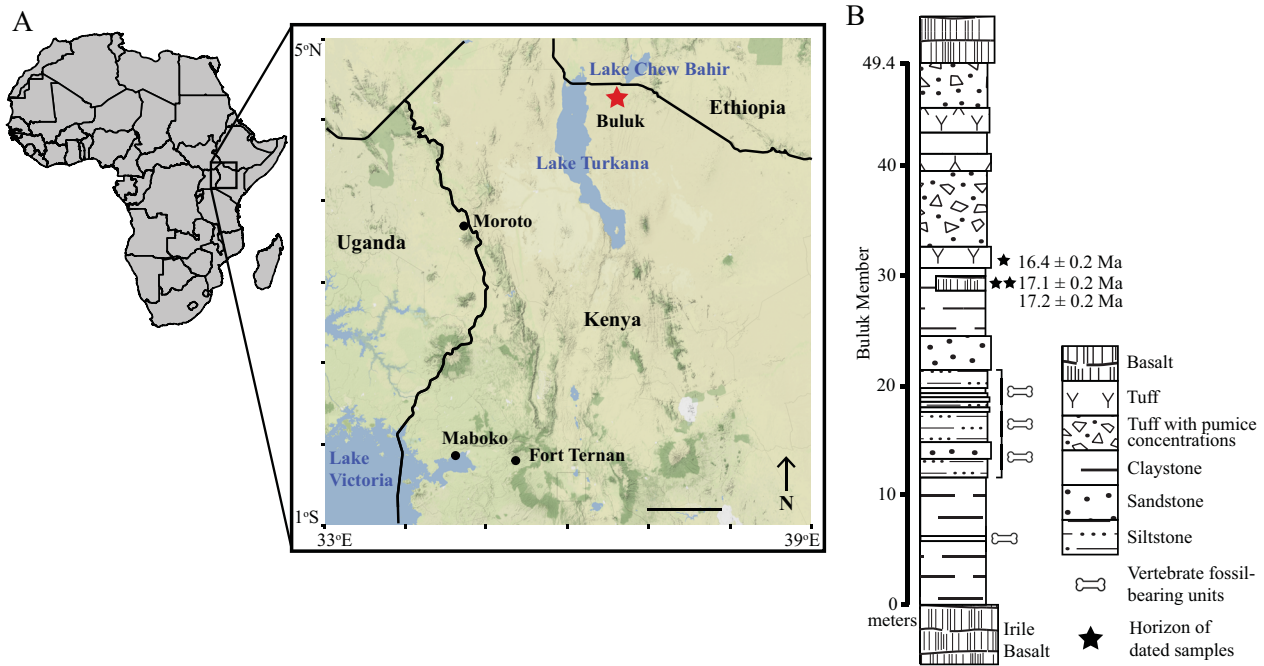


FIGURE 1. (A) Geographic map of East Africa with the location of Buluk indicated by the red star. The location of sites with comparative data included in these analyses, Moroto, Maboko, and Fort Ternan, are indicated by black circles. (B) Simplified stratigraphic column of the Bakate Formation, adapted from McDougall and Watkins (1985) and Watkins (1989).

among presumed C₃-dominated feeders before the spread of C₄ grasslands at 10 Ma. Together with information from Buluk, these four enamel carbon isotope datasets will provide a snapshot of the temporal and spatial habitat variation across three distinct regions in the developing East African Rift Valley System during the early to middle Miocene.

BACKGROUND

Geology and Fauna

Buluk is a late Early Miocene fossil site in northern Kenya, situated between Lake Turkana and Lake Chew Bahir (Figure 1A). Fossiliferous sediments at Buluk are part of the Buluk Member of the Bakate Formation (Figure 1B), which is exposed along the uplift of the Suregai-Asille plateau (Harris and Watkins, 1974; Watkins, 1983; McDougall and Watkins, 1985). The upper section of the Buluk Member is a series of sterile, reworked pantelleritic tuffs, while the lower section includes fossiliferous channel lag deposits underlying a rhyolitic layer capped by a basalt flow (McDougall and Watkins, 1985; Hurford and Watkins, 1987). The published date of this capping basalt is 17.2 ± 0.2 Ma (McDougall and Watkins, 1985). At the time of fossil deposition, the landscape at Buluk was domi-

nated by a mature river system associated with an extensive floodplain (Watkins, 1989).

Buluk preserves a rich mammalian fauna (Table 1) including proboscideans, hyracoids, primates, carnivorans, hyaenodonts, rhinocerotids, suroids (i.e., sanitheriids and suids), tragulids, and pecorans (e.g., giraffoids, bovids). Since the initial publication of Early Miocene fossils from Buluk (Harris and Watkins, 1974), ongoing fieldwork has led to the collection of >1500 mammalian fossils, prompting several lineage-specific revisions of the fauna (Geraads et al., 2013; Locke et al., 2020; Morlo et al., 2021; Nishimura et al., 2022). The taxonomic composition of the mammalian fauna from Buluk largely overlaps with many other Early Miocene East African localities, with a few taxa hinting at affinities with Middle Miocene faunas. This is most apparent in the artiodactyls – a group that shows marked taxonomic and gradistic changes during the Miocene. The ruminant artiodactyl community at Buluk is like many other Early Miocene sites, being comprised primarily of tragulids in the genus *Dorcatherium*, the giraffid *Canthumeryx*, and multiple species of small-bodied pecorans of unknown familial status (Cote, 2010; Cote et al., 2018). Buluk lacks the more derived artiodactyl families found at Middle Miocene localities like Fort Ternan and Maboko (e.g., climacoceratid giraf-

TABLE 1. Taxon list (compiled from Leakey and Walker, 1985; van der Made, 1996; Leakey et al., 2011; Geraads and Miller, 2013; Morlo et al., 2020; Sanders et al. in prep, E.M.L and E.R.M. pers obs).

Order	Family	Taxon	Isotopic Sampling
Primates	Catarrhini (Family incertae sedis)	<i>Afropithecus turkanensis</i> Catarrhini spp. <i>Noropithecus bulukensis</i>	
Carnivora	Amphicyonidae	<i>Cynelos jitu</i> <i>Cynelos macrodon</i>	
	Viverridae	cf. <i>Miopriodon</i>	
	Feliformia	Feliformia indet.	
	(Family incertae sedis)		
Hyaenodonta		<i>Hyainailouros sulzeri</i> <i>Hyainailouros</i> cf. <i>napakensis</i> Hyaenodonta indet.	
Cetartiodactyla	Anthracotheriidae	cf. <i>Sivameryx africanus</i>	Yes
	Suidae	<i>Lopholistriodon pickfordi</i> cf. <i>Kenyasus rusingensis</i> <i>Megalochoerus marymuunguiae</i>	
	Sanitheriidae	<i>Diamantohyus africanus</i>	Yes
	Tragulidae	<i>Dorcatherium pigotti</i> <i>Dorcatherium chappuisi</i>	Yes
	Pecora	<i>Canthumeryx sirtensis</i>	Yes
	(Family incertae sedis)	cf. <i>Propaleoryx nyanzae</i> Pecora indet.	
Perissodactyla	Rhinocerotidae	<i>Brachypotherium minor</i>	Yes
		Rhinocerotidae sp.	Yes
Hyracoidea	Titanohyracidae	<i>Afrohyrax championi</i>	Yes
Proboscidea	Deinotheriidae	<i>Prodeinotherium hobleyi</i>	Yes
	Mammutidae	<i>Zygolophodon</i> sp. nov.	Yes
	Gomphotheriidae	<i>Archaeobelodon</i> sp. nov. <i>Gomphotherium</i> sp.	Yes
		<i>Protanancus</i> sp. nov.	Yes
		<i>Afrochoerodon kisumuensis</i>	Yes
	Family indet.	Elephantimorph indet.	Yes

foids, bovids, and hippopotamids), but shares with Maboko two closely related species of suids in the genus *Lopholistriodon* and *Megalochoerus* (Retallack et al., 2002; Pickford, 2006).

The diverse community of fossil primates from Buluk includes the large-bodied hominoid *Afropithecus turkanensis* (Leakey and Walker, 1985; Leakey and Walker, 1997), a small-bodied non-cercopithecoid catarrhine comparable in size to *Simiolus enjessi* (Rose et al., 1992; Leakey et al., 2011;

Nishimura et al., 2022) and at least two other as-yet-undescribed non-cercopithecoid catarrhine taxa (E.M.L. and E.R.M. personal observations). Buluk has also yielded numerous fossils of the stem cercopithecoid *Noropithecus bulukensis* (Leakey, 1985; Miller et al., 2009; Locke et al., 2020). In contrast to many Early Miocene sites, where cercopithecoids are scarce or absent, *N. bulukensis* comprises roughly half of all primate fossils recovered from Buluk (Locke et al., 2020).

Stable Carbon Isotopes

The ratio of stable carbon isotopes $^{13}\text{C}/^{12}\text{C}$ (often described as $\delta^{13}\text{C}$, see 'Materials and Methods' for equations) in plants consumed by herbivores is recorded in organismal tissues during development (Lee-Thorp et al., 1989, 1991; Cerling and Harris, 1999; Sponheimer et al., 2003). The high hydroxyapatite content of tooth enamel makes it resistant to diagenetic alteration during the fossilization process, making stable carbon isotope values from fossil herbivore enamel ($\delta^{13}\text{C}_{\text{enamel}}$) a valuable tool for dietary inference of extinct taxa and paleoenvironmental reconstruction (e.g., Bocherens et al., 1996; Cerling et al., 1997; 2003a, b; Schoeninger et al., 2003; Kingston and Harrison, 2007; Levin et al., 2008; Uno et al., 2011, 2018; Cerling et al., 2015; Du et al., 2019; Paquette and Drapeau, 2021; Robinson, 2021).

The utility of $\delta^{13}\text{C}_{\text{enamel}}$ values derives from the fact that the $\delta^{13}\text{C}$ composition of vegetation consumed by herbivores reliably discriminates between the C_3 and C_4 photosynthetic pathways used by plant groups for producing chemical energy. In modern eastern African ecosystems, woody vegetation and high-elevation grasses utilize the C_3 photosynthetic pathway, which discriminates against the heavier ^{13}C and results in lower $\delta^{13}\text{C}$ values (-36‰ to -23‰) (Tieszen et al., 1979; Young and Young, 1983; Cerling and Harris, 1999). C_4 vegetation includes low-elevation grasses, sedges, and some shrubs, which have relatively higher $\delta^{13}\text{C}$ values (-14‰ to -10‰) (Tieszen et al., 1979; Young and Young, 1983; Cerling and Harris, 1999). The C_4 pathway also discriminates against ^{13}C but at a lower degree than the C_3 photosynthetic pathway.

Variation in environmental and physiological factors that influence $\delta^{13}\text{C}$ values in plants results in a greater range of $\delta^{13}\text{C}$ values for C_3 plants than for C_4 plants, reflecting a greater influence of environmental conditions on carbon isotope values using the C_3 photosynthetic pathway. For example, the lowest $\delta^{13}\text{C}$ values among C_3 plants occur in closed canopy forests due to the recycling of ^{13}C -depleted CO_2 from soil respiration in the forest understory (Vogel, 1978; Ehleringer et al., 1986; van der Merwe and Medina, 1989, 1991). C_3 plant parts found higher in the canopy and in more open canopy environments, where there is more exposure to solar radiation or more xeric conditions, have more positive $\delta^{13}\text{C}$ values (e.g., Ehleringer et

al., 1986; Heaton, 1999; Kohn, 2010). The $\delta^{13}\text{C}$ ratios of C_3 plants are also negatively correlated with mean annual precipitation (MAP), meaning plants from lower precipitation environments exhibit higher $\delta^{13}\text{C}$ values. (Kohn, 2010).

Stable Oxygen Isotopes

In conjunction with $\delta^{13}\text{C}_{\text{enamel}}$ values, the stable oxygen isotope values of herbivore tooth enamel ($\delta^{18}\text{O}_{\text{enamel}}$) can provide additional insights into aspects of an animal's diet and interactions with the environment. Environmental factors such as variation in temperature, humidity, and precipitation influence $\delta^{18}\text{O}$ values in drinking water and water within plant material, resulting in a downstream effect on $\delta^{18}\text{O}_{\text{enamel}}$ values of mammalian herbivores (Dansgaard, 1964; Rozanski et al., 1993; Higgins and McFadden, 2004). In addition to environmental variation and the $\delta^{18}\text{O}$ composition of atmospheric oxygen, the drinking habits, physiology, and metabolic mechanisms of an animal also influence its $\delta^{18}\text{O}_{\text{enamel}}$ values (Bryant and Froelich, 1995; Kohn et al., 1996, 1998; Kohn and Law, 2006; Sponheimer and Lee-Thorp, 1999; Levin et al., 2006). This confluence of biotic and abiotic factors complicates the interpretation of $\delta^{18}\text{O}_{\text{enamel}}$ values.

Despite the intricacies involved in the oxygen flux within herbivore tissues, some general patterns have emerged from the literature. Plant tissue $\delta^{18}\text{O}$ values are especially sensitive to changes in local temperature, humidity, and evapotranspiration (Sternberg et al., 1989). The $\delta^{18}\text{O}_{\text{enamel}}$ values of herbivores that rely on plant resources to obtain their water (i.e., non-obligate drinkers) track local variation in humidity and evapotranspiration due to canopy height (Kohn et al., 1996; Levin et al., 2006; Krigbaum et al., 2013; Nelson, 2013; Carter and Bradbury, 2016; Blumenthal et al., 2017; Green et al., 2022). Even the extent of folivory might influence $\delta^{18}\text{O}_{\text{enamel}}$ values (Carter and Bradbury, 2016; see also Fannin and McGraw, 2020). Herbivores that rely on drinking from local water sources for their water intake (i.e., obligate drinkers) track the $\delta^{18}\text{O}$ of meteoric water more closely, and their $\delta^{18}\text{O}_{\text{enamel}}$ values are depleted in ^{18}O relative to those of non-obligate drinkers (Levin et al., 2006). Occupying an aquatic or semi-aquatic niche also affects $\delta^{18}\text{O}_{\text{enamel}}$ values, with aquatic and semi-aquatic taxa having lower $\delta^{18}\text{O}_{\text{enamel}}$ values relative to terrestrial herbi-

vores (Cerling et al., 2003b; Levin et al., 2006; Kingston and Harrison, 2007; Clementz et al., 2008).

MATERIALS AND METHODS

Enamel Sampling

Samples of fossil tooth enamel ($n=67$) were collected from the postcanine teeth of 12 genera of non-primate mammalian herbivores from Buluk (Table 1). These samples represent a phylogenetically and ecologically diverse set of mammals including Hyracoidea, Proboscidea (Deinotheriidae, Gomphotheriidae, Mammutidae), Perissodactyla (Rhinocerotidae), and Artiodactyla (Anthracotheriidae, Giraffidae, Suidae, Sanitheriidae). Proboscidean specimens were identified by William Sanders, while all other previously unpublished specimens were identified by E.M.L and E.R.M. All specimens sampled for this study are housed in the collections of the National Museums of Kenya (NMK) in Nairobi, Kenya, and the Turkana Basin Institute (TBI) in Ileret, Kenya. All sampling was conducted with prior authorization from the NMK and by the Kenyan National Commission for Science, Technology, and Innovation (NACOSTI).

Sampling protocols were restricted to fragmentary or damaged teeth, which limits the identification of some specimens to higher taxonomic levels. Non-deinotheriid proboscidean teeth that could not be identified as gomphotheriid or mammutid were classified as “Elephantimorph indet.”. Rhinocerotid teeth that could not confidently be assigned to *Brachypotherium minor* were designated as “Rhinocerotidae indet.”, given evidence for the presence of multiple rhinocerotid taxa at Buluk (Geraads and Miller, 2013). These higher taxonomic level groups potentially include specimens representing multiple genera. For the entire sample, 75% were identified to the species level, 9% were identified to genus, and 16% were identified to superfamily (Elephantoidea) and family (Rhinocerotidae). When possible, enamel was collected from molars, specifically second and third molars, to ensure adult diet was captured.

Prior to sampling, fossil teeth were inspected for a suitable sampling surface along a broken face that would not interfere with occlusal surface morphology. The enamel surface was cleaned using a tungsten-carbide bur bit to remove matrix, cementum, and/or dentin before samples of pure enamel were removed. The mass of enamel collected reflects a compromise between obtaining a suffi-

cient volume of enamel powder for analysis while preserving informative tooth morphology. Approximately 5 or more milligrams of enamel were collected for most taxa, except for those with small or thinly enameled dentitions (i.e., Tragulidae, Hyracoidea, and Sanitheriidae), for which samples were limited to a maximum of 3 mg.

Pretreatment and Isotopic Analysis

Following Uno and colleagues (2011), a subset of enamel samples ($n=15$) was analyzed with and without pretreatment to determine the effect of treatment on $\delta^{13}\text{C}_{\text{enamel}}$ values. Enamel powder samples with a mass >6 mg were selected for pretreatment/treatment comparisons. Pretreatment was performed at the Paleoecology Lab at the University of Michigan. Samples undergoing pretreatment were soaked in 3% sodium hypochlorite (NaOCl) for 12 hours. Samples were centrifuged and NaOCl was decanted using a pipette without disturbing the enamel pellet. Enamel powder was rinsed with deionized water to neutrality. Samples were then treated with 0.1M solution of acetic acid (CH_3COOH) for 12 hours and rinsed with deionized water to neutrality. The enamel powder pellet was transferred to a glass vial and excess moisture was removed by freeze drying overnight. Results of treated versus untreated Buluk $\delta^{13}\text{C}_{\text{enamel}}$ and $\delta^{18}\text{O}_{\text{enamel}}$ values are shown in Appendix 1. The difference in $\delta^{13}\text{C}_{\text{enamel}}$ and $\delta^{18}\text{O}_{\text{enamel}}$ values between treated and untreated samples was less than $\pm 0.6\text{\textperthousand}$ for all 15 samples, indicating a minimal effect of treatment (Appendix 2).

Since a considerable amount of sample powder can be lost during pretreatment, standard protocols are to generally leave samples with $\sim 1\text{--}4$ mg of enamel powder untreated and to convert their values to match pretreated samples using regression equations (e.g., Levin et al., 2008; Cerling et al., 2015). Here, based on the results shown in Appendix 1, all other untreated samples were converted to match pretreated samples using the respective carbon and oxygen regression equations:

$$\delta^{13}\text{C}_{\text{final}} = 0.96 * \delta^{13}\text{C}_{\text{untreated}} - 0.67, R^2 = 0.97 \quad (1)$$

$$\delta^{18}\text{O}_{\text{final}} = 0.99 * \delta^{18}\text{O}_{\text{untreated}} - 0.26, R^2 = 0.96 \quad (2)$$

Treated and untreated samples were sent to the University of Florida, Department of Geosciences Light Stable Isotope Mass Spec Lab for analysis and determination of $^{13}\text{C}/^{12}\text{C}$ ratios. In glass vials, 3–5 mg of enamel powder sample and NBS-19 standards were reacted with 99% phos-

phoric acid (H_3PO_4) at 70°C. The CO_2 produced from this reaction was analyzed using mass spectrometry with a Kiel III carbonate preparation device coupled with a Finnigan-Mat 252 isotope ratio mass spectrometer. The standard deviation for NBS-19 standard analyses was ~0.03‰ for $\delta^{13}\text{C}$ and ~0.07‰ for $\delta^{18}\text{O}$. Results are reported in standard parts per million notation (‰):

$$\delta^{13}\text{C} = (\delta^{18}\text{O}) = (R_{\text{sample}}/R_{\text{standard}} - 1) * 1,000 \quad (3)$$

$$R = ^{13}\text{C}/^{12}\text{C} \text{ or } ^{18}\text{O}/^{16}\text{O} \quad (4)$$

Interpretation of Enamel Stable Isotope Ratios

The $\delta^{13}\text{C}$ value of atmospheric CO_2 ($\delta^{13}\text{C}_{\text{atm}}$) that is incorporated into plant tissues fluctuates through time and thus impacts the $\delta^{13}\text{C}$ values of plant tissues. This flux in $\delta^{13}\text{C}_{\text{atm}}$ values must be standardized before comparing $\delta^{13}\text{C}_{\text{enamel}}$ values from different time periods. Since the Industrial Revolution (estimated to be approximately A.D. 1750), the generation of ^{13}C -depleted CO_2 from anthropogenic processes has decreased global $\delta^{13}\text{C}_{\text{atm}}$ values (Francey et al., 1999). During the early and Middle Miocene, estimated average $\delta^{13}\text{C}_{\text{atm}}$ values from North Atlantic benthic foraminifera varied between -4.8‰ to -6.6‰ (Tipple et al., 2010). A pre-Industrial Revolution $\delta^{13}\text{C}_{\text{atm}}$ value of -6.3‰ ($\delta^{13}\text{C}_{1750}$) was used to standardize fossil enamel carbon isotope values and any modern enamel carbon isotope values mentioned in the text.

For the Early Miocene age (17.2±0.2 Ma, McDougall and Watkins, 1985), the $\delta^{13}\text{C}_{\text{atm}}$ values for 17.0 - 17.4 Ma from the high-resolution benthic dataset from Tipple et al. (2010) were averaged (mean = -5.66‰). Therefore, -0.64‰ was added to $\delta^{13}\text{C}_{\text{enamel}}$ values for standardization to $\delta^{13}\text{C}_{1750}$ values. Recently published paleoecological work has placed the age of Buluk closer to 16 Ma (Peppe et al., 2023). However, this relies on radiometric K-Ar (alkali feldspar) and fission-track (zircon) ages of 16.1± 0.2 Ma from the volcaniclastic tuffs overlying the Bakate Formation (Figure 1B; Watkins, 1989; Hurford and Watkins, 1987). We conservatively retain the use of the 17.2 Ma date to standardize enamel samples from Buluk with modern and other fossil carbon isotope data. For completeness, a comparison of the differences in $\delta^{13}\text{C}_{\text{enamel}}$ value correction using a date of 16 Ma

versus 17.2 Ma is provided in Appendix 3. All fossil and modern $\delta^{13}\text{C}_{\text{enamel}}$ results are reported as $\delta^{13}\text{C}_{1750}$ values to accommodate fluctuations in atmospheric $\delta^{13}\text{C}$ so modern and fossil enamel isotopic values can be compared. Published $\delta^{13}\text{C}_{\text{enamel}}$ values from Moroto, Maboko, and Fort Ternan were also corrected using the high-resolution benthic $\delta^{13}\text{C}_{\text{atm}}$ estimates from Tipple et al. (2010) as follows: raw Maboko $\delta^{13}\text{C}_{\text{enamel}}$ values were corrected following Arney et al., (2022); for the interval of 13.40-14.0 Ma (mean $\delta^{13}\text{C}_{\text{atm}} = -5.48\text{\textperthousand}$), -0.82‰ was added to published Fort Ternan $\delta^{13}\text{C}_{\text{enamel}}$ values; for the interval of 20.71-21.38 Ma (mean $\delta^{13}\text{C}_{\text{atm}} = -6.04\text{\textperthousand}$), -0.26‰ was added to published Moroto $\delta^{13}\text{C}_{\text{enamel}}$ values.

Isotopic dietary ranges that correspond with general biomes were used to assess habitat structure among presumed C_3 -dominated ecosystems (closed canopy vs. open canopy; mesic vs. xeric conditions). The following dietary categories are modified from the diet classifications described in Cerling and colleagues (2015): C_3 closed canopy diets are defined as those with $\delta^{13}\text{C}_{\text{enamel}}$ values < -14‰; C_3 open canopy diets are defined as those with $\delta^{13}\text{C}_{\text{enamel}}$ values between -14‰ and -8‰; and C_3/C_4 mixed diets are characterized as those with $\delta^{13}\text{C}_{\text{enamel}}$ values > -8‰.

All statistical analyses and plots were made using R (version 4.2.1, R Core Team, 2021). $\delta^{13}\text{C}_{\text{enamel}}$ data from Buluk was compared with published enamel stable isotope values from fossil mammals from Moroto (MacLatchy et al., 2023), Maboko (Arney et al., 2002) and Fort Ternan (Cerling et al., 1997) (Table 2). Shapiro-Wilk tests indicate a normal distribution for $\delta^{13}\text{C}_{\text{enamel}}$ data from Buluk, Maboko, and Fort Ternan, but not from $\delta^{13}\text{C}_{\text{enamel}}$ data Moroto. Intersite $\delta^{13}\text{C}_{\text{enamel}}$ comparisons were conducted using pairwise nonparametric Mann-Whitney U tests. Bulk $\delta^{18}\text{O}_{\text{enamel}}$ values between localities were not statistically compared, since each locality has a unique meteoric water source(s) with unknown $\delta^{18}\text{O}$ values, which can further complicate interpretations. Results of the intersite carbon analysis and oxygen comparisons are reported in the main text of the Discussion.

RESULTS

General Patterns

Buluk herbivore $\delta^{13}\text{C}_{\text{enamel}}$ values range from $-12.7\text{\textperthousand}$ to $-9.3\text{\textperthousand}$ with a mean value of $-11.2\text{\textperthousand}$ (Figure 2; Table 2). These values are consistent with herbivores foraging in a C_3 -dominated open canopy woodland ecosystem. Carbon isotopic profiles from Buluk herbivores do not fall within the range of values for closed canopy understory foraging, suggesting closed canopy habitats were either absent from the landscape or were not utilized consistently by herbivores sampled here. There is no evidence for the consumption of C_4 resources, even in low proportions.

The $\delta^{18}\text{O}_{\text{enamel}}$ values from Buluk range from $-6.4\text{\textperthousand}$ to $+3.5\text{\textperthousand}$ (Figure 3). Differences in $\delta^{18}\text{O}_{\text{enamel}}$ values among taxa potentially reflect variation in water intake strategies, physiological water flux, changes in meteoric water $\delta^{18}\text{O}$ values due to environmental factors, and/or contributions from multiple water sources. While it is difficult to make specific inferences about drinking habits or environmental conditions given the lack of extant analogs for many of the fossil taxa sampled here, documenting intra and inter-specific variation in $\delta^{18}\text{O}_{\text{enamel}}$ values is valuable for future comparative work. Taxon-specific summary statistics for $\delta^{13}\text{C}_{\text{enamel}}$ and $\delta^{18}\text{O}_{\text{enamel}}$ are

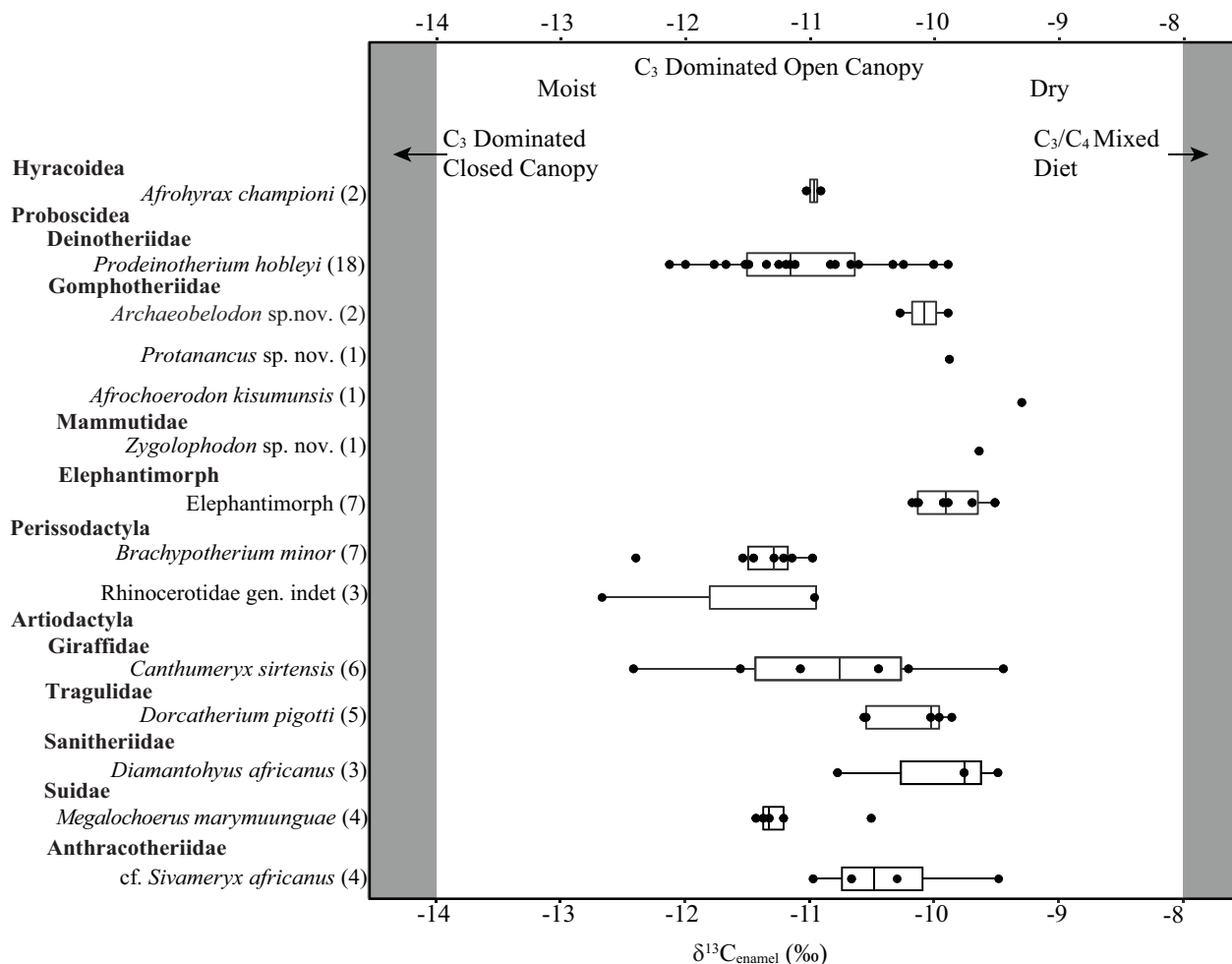


FIGURE 2. Buluk $\delta^{13}\text{C}_{\text{enamel}}$ value boxplots arranged by taxonomic guild. Vertical lines in a boxplot represent the median, box ends indicate the 1st and 3rd quartiles, and horizontal lines define the range of values except for outliers. The shaded region to the left denotes values for feeding in closed canopy forest while the shaded region to the right indicates mixed C_3/C_4 diets. The non-shaded region designates values from open canopy foraging. Sample sizes are in parentheses.

TABLE 2. Fossil sites compared in this study.

Site	Age	Mean $\delta^{13}\text{C}_{\text{enamel}}$	Median $\delta^{13}\text{C}_{\text{enamel}}$	SD
Moroto ^a	21 Ma	-10.4	-10.3	1.6
Buluk	17.2 Ma	-10.7	-10.8	0.8
Maboko ^b	~16-13.7 Ma ^c	-12	-12	1
Fort Ternand ^d	13.7 Ma ^e	-11.7	-11.8	1

^a $\delta^{13}\text{C}_{\text{enamel}}$ values and age from MacLatchy et al., (2023)

^b $\delta^{13}\text{C}_{\text{enamel}}$ values from Arney et al., (2022)

^c Age from Feibel and Brown (1991)

^d $\delta^{13}\text{C}_{\text{enamel}}$ values from Cerling et al., (1997)

^e Age from Pickford et al., (2006)

reported Table 3, and these values are plotted together for completeness in Appendix 4.

Hyracoidea

Two *Afrohyrax championi* teeth were sampled in this study, with $\delta^{13}\text{C}_{\text{enamel}}$ values of -11.0‰. These values overlap with the $\delta^{13}\text{C}_{\text{enamel}}$ values of several Buluk taxa, including deinotheres, the giraffid *Canthumeryx sirtensis*, the upper range of rhinocerotid values, and the low end of values for the anthracotheriid cf. *Sivameryx africanus* (Figure 2). $\delta^{18}\text{O}_{\text{enamel}}$ values of the two *A. championi* specimens are -0.1‰ and +1.6‰. These oxygen isotopic values are relatively high, overlapping with cf. *S. africanus*, *C. sirtensis*, and the large-bodied suid *Megalchoerus marymuunguae* (Figure 3).

Proboscidea

The $\delta^{13}\text{C}$ values for all sampled Buluk proboscideans range from -12.1‰ to -9.3‰ (Figure 2; Table 3). The range of $\delta^{13}\text{C}$ values for *Prodeinotherium hobleyi* is -12.1‰ to -9.9‰, consistent with prior isotopic analyses from Buluk showing a pure C₃ browsing signal for this taxon (Cerling et al., 1999). The range for the elephantimorph taxa (i.e., gomphtheriids and mammutids) is -10.7‰ to -9.5‰, suggesting that they may have fed on more water-stressed browse than the relatively $\delta^{13}\text{C}$ depleted deinotheriid. These differences could also be the result of body size variation (Tejada-Lara et al., 2018), plant parts consumed (Carlson and Kingston, 2014; Blumenthal et al., 2016), and interspecific physiological and metabolic variation (Cerling et al., 2021).

The $\delta^{18}\text{O}_{\text{enamel}}$ values of Buluk proboscideans range from -6.4‰ to -0.2‰, with a mean value of -3.1‰ (Figure 3). Oxygen signatures for the five proboscidean taxa overlap extensively, with the

range of $\delta^{18}\text{O}_{\text{enamel}}$ values of *P. hobleyi* encompassing all other proboscidean values. Overall, the lowest $\delta^{18}\text{O}_{\text{enamel}}$ values of all taxa are from elephantimorph proboscideans and *P. hobleyi* specimens, suggesting proboscideans were dependent on drinking water from a variety of sources (e.g., rivers, springs, ponds, or lakes) for water intake. Proboscideans are the most $\delta^{18}\text{O}$ depleted group of mammals sampled from Buluk.

Rhinocerotidae

Ten rhinocerotid teeth were sampled: seven belonging to *Brachypotherium minor* and three assigned to Rhinocerotidae gen. indet., which may represent a distinct species (Geraads and Miller, 2013). $\delta^{13}\text{C}_{\text{enamel}}$ values for the total Rhinocerotidae sample range from -12.7‰ to -11.0‰. The range in *B. minor* $\delta^{13}\text{C}_{\text{enamel}}$ values is from -12.4‰ to -11.0‰, which is bracketed by the Rhinocerotidae gen. indet. values (Figure 2). The rhinocerotid carbon isotope values overlap with those from the suid *M. marymuunguae*, the giraffid *C. sirtensis*, and the deinotheriid *P. hobleyi*, and are lower than $\delta^{13}\text{C}$ values of the sanitheriid *Diamantohyus africanus*, the tragulid *Dorcatherium pigotti*, the anthracothere cf. *S. africanus*, and all elephantimorph proboscideans.

Rhinocerotid $\delta^{18}\text{O}_{\text{enamel}}$ values range from -3.6‰ to +0.2‰ and have a mean value of -1.3‰ (Figure 3). These oxygen isotope values are higher than most $\delta^{18}\text{O}_{\text{enamel}}$ samples from elephantimorph proboscideans and lower than most samples from *C. sirtensis*.

Giraffidae

Six *Canthumeryx sirtensis* teeth were sampled from Buluk. $\delta^{13}\text{C}_{\text{enamel}}$ values for *C. sirtensis*

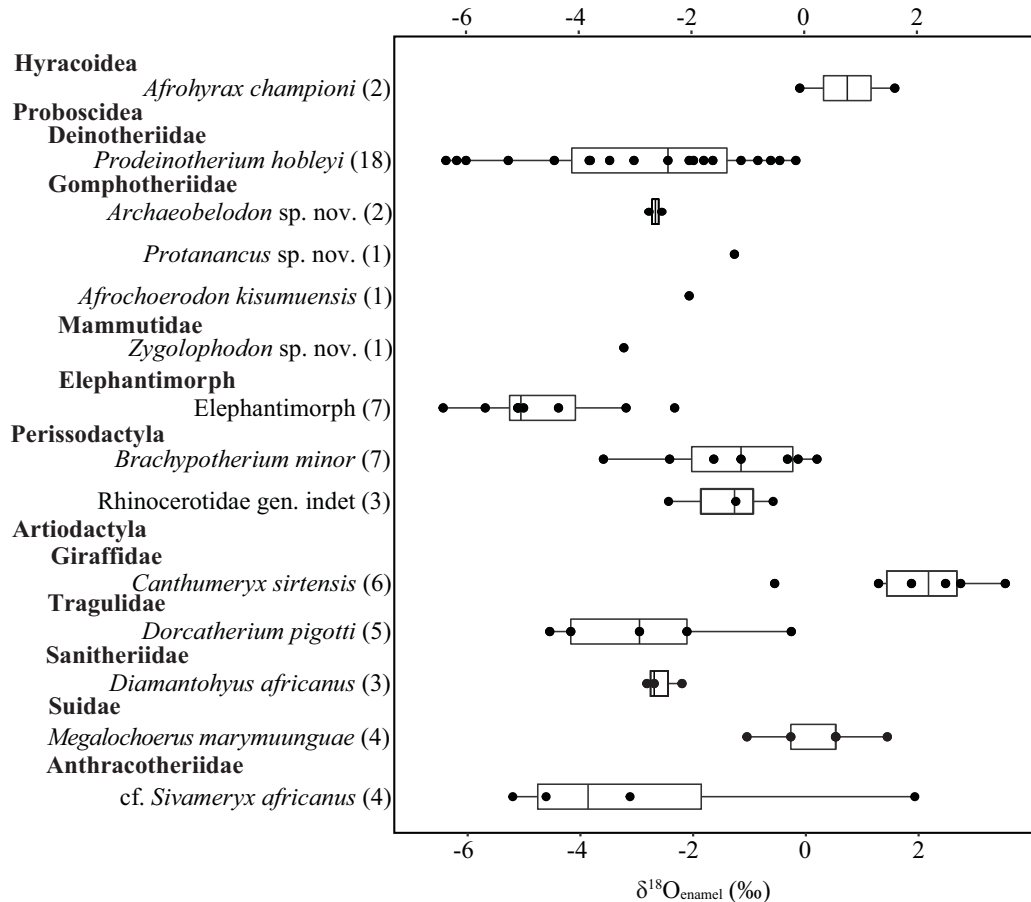


FIGURE 3. Buluk $\delta^{18}\text{O}_{\text{enamel}}$ value boxplots arranged by taxonomic guild. Sample sizes are in parentheses.

range from $-12.4\text{\textperthousand}$ to $-9.4\text{\textperthousand}$ and have a mean value of $-10.9\text{\textperthousand}$ (Figure 2). *C. sirtensis* has the highest range of $\delta^{13}\text{C}_{\text{enamel}}$ values among all sampled mammals from Buluk, which suggests that this taxon has a relatively broad dietary range.

The $\delta^{18}\text{O}_{\text{enamel}}$ values for *C. sirtensis* range from $-0.6\text{\textperthousand}$ to $+3.5\text{\textperthousand}$, which is relatively enriched in ^{18}O compared to all other taxa (Figure 3). Extant giraffes in many modern assemblages are similarly enriched relative to other herbivores on the landscape (Kingston and Harrison, 2007; Kohn et al., 1996; Sponheimer and Lee-Thorp, 1999). The ^{18}O enriched *C. sirtensis* values are consistent with this taxon preferentially relying on diet for water intake, like extant *Giraffa* (Levin et al., 2006). These results also indicate *C. sirtensis* browsed on dietary items enriched in ^{18}O , such as leaves and/or fruit from high in the woody canopy (Krigbaum et al., 2013; Carter and Bradbury, 2016; Roberts et al., 2017).

Tragulidae

The $\delta^{13}\text{C}_{\text{enamel}}$ values for the five *Dorcatherium pigotti* teeth sampled range from $-10.6\text{\textperthousand}$ to $-9.9\text{\textperthousand}$ and have a mean value of $-10.2\text{\textperthousand}$ (Figure 2). This range of $\delta^{13}\text{C}_{\text{enamel}}$ values overlaps with many other artiodactyls from Buluk, including *Di. africanus*, cf. *S. africanus*, and *C. sirtensis*. The *D. pigotti* carbon isotopic results are ^{13}C enriched relative to the limited $\delta^{13}\text{C}_{\text{enamel}}$ data available for the forest-dwelling, extant African tragulid, *Hyemoschus aquaticus* ($-13.9\text{\textperthousand}$; Cerling et al., 2004), indicating *D. pigotti* browsed in more open wooded habitats. There is a second, larger-bodied tragulid species present at Buluk, *Dorcatherium chappuisi* (Table 1), which could not be sampled. At the Middle Miocene site of Maboko, where these two taxa also co-occur, *D. chappuisi* is more enriched in ^{13}C than *D. pigotti*, but whether these taxa exhibit similar niche partitioning at Buluk cannot be determined at this time.

TABLE 3. Summary statistics for $\delta^{13}\text{C}_{\text{enamel}}$ and $\delta^{18}\text{O}_{\text{enamel}}$.

Taxa	N	$\delta^{13}\text{C}_{\text{enamel}} (\text{\textperthousand})$					$\delta^{18}\text{O}_{\text{enamel}} (\text{\textperthousand})$				
		Mean	Median	Min	Max	Mean	Median	Min	Max		
Hyracoidea											
<i>Afrohyrax championi</i>	2	-11.4	-11.4	-11.5	-11.4	0.7	0.7	-0.1	1.6		
Deinotheriidae											
<i>Prodeinotherium hobleyi</i>	19	-11.5	-11.6	-12.6	-10.4	-2.9	-2.4	-6.4	-0.2		
Gomphotheriidae											
<i>Archaeobelodon</i> sp. nov.	2	-10.5	-10.5	-10.7	-10.4	-2.7	-2.7	-2.8	-2.6		
<i>Afrochoerodon kisumuensis</i>	1	-9.8	-9.8	-	-	-2.1	-2.1	-	-		
<i>Protanancus</i> sp. nov.	1	-10.3	-10.3	-	-	-1.3	-1.3	-	-		
Mammalidae											
<i>Zygodipodon</i> sp. nov.	1	-10.1	-10.1	-	-	-3.2	-3.2	-	-		
Elephantimorph											
<i>Elephantimorph</i>	8	-10.3	-10.4	-10.6	-10	-4.7	-5.1	-6.4	-2.3		
Rhinocerotidae											
<i>Brachypotherium minor</i>	7	-11.9	-11.8	-12.9	-11.4	-1.3	-1.2	-3.6	0.2		
<i>Rhinocerotidae</i> sp.	3	-12	-11.4	-13.1	-11.4	-1.5	-1.3	-2.5	-0.6		
Giraffidae											
<i>Canthumeryx sirtensis</i>	6	-11.3	-11.2	-12.9	-9.9	1.9	2.2	-0.6	3.5		
Tragulidae											
<i>Dorcatherium</i> cf. <i>pigotti</i>	5	-10.7	-10.5	-11	-10.3	-2.8	-3	-4.5	-0.3		
Sanitheriidae											
<i>Diamantohyus africanus</i>	3	-10.5	-10.2	-11.2	-10	-2.6	-2.7	-2.8	-2.2		
Suidae											
<i>Megalochoerus marymuunguae</i>	5	-11.6	-11.8	-11.9	-11	0.2	0.5	-1	1.4		
Anthracotheriidae											
cf. <i>Sivameryx africanus</i>	4	-10.8	-10.9	-11.1	-10.8	-2.7	-3.9	-5.2	-4.6		

D. pigotti $\delta^{18}\text{O}_{\text{enamel}}$ values range from -4.5‰ to -0.3‰ and have a mean value of -2.8‰. The distribution of *D. pigotti* overlaps with the distribution of $\delta^{18}\text{O}_{\text{enamel}}$ values for deinotheres, the higher values of elephantimorphs, the lower values of rhinocerotids, and all other artiodactyls from Buluk (Figure 3).

Suoidea

Suid species sampled here include three specimens of the sanithe *Diamantohyus africanus* and five specimens of the large-bodied suid *Megalochoerus marymuunguae*. Two smaller-bodied suids, *Lopholistriondon pickfordi* and cf. *Kenya-sus rusingensis*, are also present at Buluk (Table 1) but could not be sampled. *D. africanus* $\delta^{13}\text{C}_{\text{enamel}}$ values range from -10.8‰ to -9.5‰ and have a mean value of -10.0‰ (Table 3). These carbon isotopic values are ^{13}C enriched compared to $\delta^{13}\text{C}_{\text{e-}}$

namel values from *M. marymuunguae* (Figure 2), which range from -11.4‰ to -10.5‰ and have a mean value of -11.2‰. The lower $\delta^{13}\text{C}_{\text{enamel}}$ values of *M. marymuunguae* indicate it may have had a different foraging strategy than *D. africanus*, selecting plants or plant parts enriched in ^{13}C or foraging in more open canopy.

The $\delta^{18}\text{O}_{\text{enamel}}$ values for *D. africanus* range from -2.8‰ to -2.2‰ and have a mean value of -2.6‰. The $\delta^{18}\text{O}_{\text{enamel}}$ values for *M. marymuunguae* range from -1.0‰ to +1.4‰ and have a mean value of +0.2‰, which are higher than the $\delta^{18}\text{O}_{\text{enamel}}$ values of *D. africanus* (Figure 3). The ^{18}O depleted $\delta^{18}\text{O}_{\text{enamel}}$ values in *D. africanus* compared to *M. marymuunguae* oxygen profiles is consistent with a dependence on a more ^{18}O depleted diet and water sources. Differences in body size and physiological metabolic processes could also

have contributed to the divergent carbon and oxygen profiles between these two suoids (Bryant and Froelich, 1995; Kohn et al., 1996; Passey et al., 2005; Tejada-Lara et al., 2018; Cerling et al., 2021), as *D. africanus* is markedly smaller than *M. marymuunguae* (van der Made, 1996; Grossman, 2008). The higher $\delta^{18}\text{O}_{\text{enamel}}$ values for *M. marymuunguae*, however, do not follow the expectations outlined in Bryant and Froelich (1995) for a much larger species, where larger body sizes take in more liquid water and rely less on food metabolism for oxygen intake.

Anthracotheriidae

Four anthracothere teeth were sampled, which are identified as cf. *Sivameryx africanus*. Anthracothere $\delta^{13}\text{C}_{\text{enamel}}$ values range from -11.0‰ to -9.5‰ with a mean value of -10.4‰. The distribution of anthracothere $\delta^{13}\text{C}_{\text{enamel}}$ values overlaps with those of tragulids, sanitheriids, and elephantimorph proboscideans (Figure 2).

The $\delta^{18}\text{O}_{\text{enamel}}$ values for anthracotheres range from -5.2‰ to +1.9‰ and have a mean value of -2.7‰. Most anthracothere $\delta^{18}\text{O}_{\text{enamel}}$ values are depleted in ^{18}O and overlap with $\delta^{18}\text{O}_{\text{enamel}}$ values of all proboscideans and *D. pigotti*. One $\delta^{18}\text{O}_{\text{enamel}}$ value of cf. *S. africanus* is relatively ^{18}O enriched, overlapping with $\delta^{18}\text{O}_{\text{enamel}}$ values of *C. sirtensis* (Figure 3). While this sample came from a maxillary P⁴ of cf. *S. africanus*, the relatively enriched $\delta^{18}\text{O}$ enamel value likely reflects a shift in either surface water and/or dietary $\delta^{18}\text{O}$ values rather than a weaning signature, as the P4s of most extant ruminant and non-ruminant herbivores form and erupt after the permanent upper molars (Spinage, 1976; Davis, 1980; Levine, 1982; Hillman-Smith et al., 1986; Fricke and O’Niel, 1996; Kohn, 1996; Kohn et al., 1998; Fricke et al., 1998; Green et al., 2018, 2022).

DISCUSSION

Herbivore Enamel Isotopes, Diets, and Paleoecology

The range of Buluk herbivore $\delta^{13}\text{C}_{\text{enamel}}$ values (-13.1‰ to -9.8‰) indicates these mammals had C₃-dominated diets. Elephantimorph proboscideans exhibit the highest $\delta^{13}\text{C}_{\text{enamel}}$ values in the sample and rhinocerotids exhibit the lowest values (Figure 2). Stable carbon isotope data from pedogenic carbonates at Buluk indicates the presence

of a C₄ component on the landscape (Peppe et al., 2023), but evidence from $\delta^{13}\text{C}_{\text{enamel}}$ samples suggests the herbivorous mammals at Buluk were likely not consuming this resource. Using methods published by MacLatchy et al. (2023), estimated fractions of C₄ biomass at Buluk from pedogenic carbonate $\delta^{13}\text{C}$ values indicate a wide range of possible C₄ biomass, with the lowest reconstructed C₄ percentage of 19% (95% confidence interval = 0% to 46%; $\delta^{13}\text{C}_{\text{carbonate}} = -8.7\text{\textperthousand}$) and the largest reconstructed C₄ percentage of 72% (95% confidence interval = 46% to 97%; $\delta^{13}\text{C}_{\text{carbonate}} = -0.8\text{\textperthousand}$).

Due to the opportunistic nature of the sampling strategy, it remains possible that some Buluk herbivores that were unable to be sampled for this analysis did indeed utilized C₄ resources. It is also possible that the abundance of C₄ vegetation was too low to be consistently incorporated into herbivore diets, or that C₄ plants were not preferred dietary items. The tightly constrained range of $\delta^{13}\text{C}_{\text{enamel}}$ values from Buluk suggests similar foraging patterns among mammalian herbivores, or niche partitioning along axes that are not reflected in isotopic analyses (Arney et al., 2022). The overall range of herbivore $\delta^{13}\text{C}_{\text{enamel}}$ values reflects feeding in open environments without closed canopy components, water-stressed C₃ plants, or abundantly consumed C₄ plants.

These enamel carbon isotope results are consistent with many, but not all previous paleoecological findings from Buluk. Preliminary analyses of paleosol geochemistry and morphology suggest a relatively open woodland environment within a seasonal, subhumid precipitation regime (Lukens et al., 2017b, 2021). In this way, paleoenvironmental reconstructions at Buluk are consistent with the interpretation that heterogeneous open habitats were present across East Africa during the Early Miocene (Peppe et al., 2021). The fact that the Buluk herbivores exhibit C₃-dominated diets within this open canopy habitat is also consistent with previous local and regional stable isotopic work showing that East African herbivore diets were C₃-dominated prior to 10 Ma (Cerling et al., 1991, 1997; Uno et al., 2011; Feakins et al., 2013; Polissar et al., 2019).

Enamel oxygen profiles from Buluk mammals indicate variation in water intake strategies between herbivore guilds (Figure 3). The giraffid *C. sirtensis* displays the highest $\delta^{18}\text{O}_{\text{enamel}}$ values,

consistent with an interpretation of this taxon as a non-obligate drinker receiving most of its water intake from dietary vegetation, as seen in most extant giraffes (e.g., Sponheimer and Lee-Thorpe, 1999; Cerling et al., 2003a, b; Schoeninger et al., 2003; Levin et al., 2008) and $\delta^{18}\text{O}_{\text{enamel}}$ results from Maboko and Fort Ternan (Appendix 4). The lowest $\delta^{18}\text{O}_{\text{enamel}}$ values among the Buluk fauna are found in the elephantimorph proboscideans, which suggests that these taxa had a higher reliance on standing water (Levin et al., 2008). Although Buluk's depositional environment reflects a mature river system (Watkins, 1989), intra- and inter-specific variation in $\delta^{18}\text{O}_{\text{enamel}}$ values may reflect multiple sources of drinking water with varying $\delta^{18}\text{O}$ values across the landscape. It is important to note that, while $\delta^{18}\text{O}_{\text{enamel}}$ values have been used to draw inferences about obligate vs. non-obligate drinking herbivores from Plio-Pleistocene fossil localities (e.g., Blumenthal et al., 2017), the lack of modern analogs for some Early and Middle Miocene taxa makes inferences about their drinking behaviors (i.e., obligate vs. non-obligate) more tentative.

Precipitation seasonality has been previously proposed to be a driver in catarrhine evolution, specifically a shift from low to high precipitation seasonality in the Late Miocene (e.g., Temerin and Cant, 1983; Andrews and Martin, 1991; Pickford, 1995). Evidence for Miocene climatic seasonality, however, is limited both for the Turkana Basin and for eastern Africa more broadly (Green et al., 2022). The range of herbivore $\delta^{18}\text{O}_{\text{enamel}}$ values from Buluk (9.9‰, n=67) is relatively high when compared to the bulk $\delta^{18}\text{O}_{\text{enamel}}$ values of herbivores from Kalodirr (range = 7.8‰, n=66), an Early Miocene (~17 Ma) site in West Turkana where primate molar serial oxygen profiles have yielded clear evidence of seasonal precipitation variation (Green et al., 2022). While differences in $\delta^{18}\text{O}_{\text{enamel}}$ values between Kalodirr and Buluk may reflect differences in local hydrological dynamics (i.e., different sources of rainwater with different $\delta^{18}\text{O}_{\text{enamel}}$ values) and/or taxonomic sampling, the greater range of oxygen values from Buluk this provisionally could indicate that Buluk, like Kalodirr, was characterized by strong wet/dry seasonality. The frequency and intensity of wet/dry seasons at Buluk is currently unknown but may be better understood by future serial sampling of enamel from primates and/or associated fauna.

Among the Buluk herbivores, the most positive $\delta^{13}\text{C}_{\text{enamel}}$ values are from elephantimorph proboscideans (gomphotheres and mammutids). Elephantimorph $\delta^{13}\text{C}_{\text{enamel}}$ values overlap with some deinothere samples, but deinotheres exhibit a significantly larger variance in $\delta^{13}\text{C}_{\text{enamel}}$ values than elephantimorphs ($F[18,12]=4.733$, $p=0.009$), which extends into a more $\delta^{13}\text{C}$ -depleted range than any other proboscidean sampled from Buluk. This greater range of variation is likely due to the larger sample size of deinothere teeth compared to other fauna (Figure 3), which captures more isotopic variation compared with the limited samples of available gomphothere and mammutid teeth. Despite these sample size limitations, it is also possible that elephantimorph proboscideans consumed vegetation or plant parts that were enriched in $\delta^{13}\text{C}$ compared to deinotheres (Carlson and Kingston, 2014; Blumenthal et al., 2016), or that isotopic enrichment differs between these groups as a result of differences in digestive physiology, metabolism, and body size (Passey et al., 2005; Tejada-Lara et al., 2018; Cerling et al., 2021). Enamel microwear features indicate that Buluk *P. hobleyi*, *Archaeobelodon* sp. nov., and *Zygodolophodon* sp. nov. taxa likely fed on tough, fibrous browse (Sanders et al., 2020). Mesowear angles for *Archaeobelodon* sp. nov. molars suggest browsing with some mixed feeding for this species (Saarinen and Lister, 2023). Mixed feeding among elephantimorphs that incorporated C₃ browse or grasses enriched in $\delta^{13}\text{C}$ could be driving the higher $\delta^{13}\text{C}_{\text{enamel}}$ values relative to the other proboscidean taxa sampled.

There is no clear pattern of oxygen isotopic partitioning among the Buluk proboscideans based on $\delta^{18}\text{O}_{\text{enamel}}$ values. Deinothere and elephantimorph $\delta^{18}\text{O}_{\text{enamel}}$ values overlap extensively between deinotheres, gomphotheres, and mammutids (Figure 3). Deinothere $\delta^{18}\text{O}$ values are widely variable and overlap with rhinocerotids, tragulids, sanitheres, suids, and anthracotheres. This broad range of proboscidean $\delta^{18}\text{O}$ values may be related to methodology (e.g., sampling different tooth positions and areas of the crown; Kohn et al., 1996; Malone et al., 2021) or dietary ecology (e.g., drinking water from across multiple sources or consuming food sources with widely varying $\delta^{18}\text{O}$ values; Kohn et al., 1996; Carter and Bradbury, 2016).

Relatively depleted $\delta^{18}\text{O}_{\text{enamel}}$ values from early Miocene anthracotheres at Kalodirr appear to

corroborate previous inferences of an aquatic or semi-aquatic niche for this clade (Green et al., 2022), which was previously suggested based on the association of anthracothere skeletal remains with lacustrine sediments (Pickford, 1981, 1983). Extant semi-aquatic herbivores like the hippopotamus (*Hippopotamus amphibius*) have $\delta^{18}\text{O}_{\text{enamel}}$ values lower than associated terrestrial fauna (Bocherens et al., 1996; Clementz et al., 2008). This technique has been applied to fossil anthracotheres from the Eocene and Oligocene of Egypt as well as the Oligocene of Germany to infer both semi-aquatic and terrestrial niches for members of this clade (Clementz et al., 2008; Liu et al., 2008; Tütken and Absolon, 2015). In contrast with Kalodirr specimens of *Sivameryx africanus*, the Buluk specimens of cf. *Sivameryx africanus* have relatively enriched $\delta^{18}\text{O}_{\text{enamel}}$ values (Figure 3) that overlap with oxygen profiles of terrestrial herbivores from the same site (e.g., elephantimorphs, deinotheres, tragulids). One possible interpretation of these results is that cf. *Sivameryx* from Buluk was occupying a more terrestrial niche rather than the semi-aquatic one proposed for *Sivameryx* from Kalodirr.

Buluk preserves a diverse suid community that includes the small-bodied selenodont sanithere *Diamantohyus africanus*, the small-bodied lophodont suid *Lopholistriondon pickfordi* and two bunodont kubanochoerine suids, cf. *Kenyasus rusingensis* and the much larger *Megalichoerus marymuunguae* (Pickford, 1983a; van der Made, 1996; Bishop, 2010). Only *M. marymuunguae* and *D. africanus* could be sampled for this analysis (Table 1), but variation in their carbon and oxygen isotopic values suggests possible niche partitioning among the Buluk suids. *Megalichoerus marymuunguae* has lower $\delta^{13}\text{C}_{\text{enamel}}$ values than *D. africanus*, suggesting it fed on more ^{13}C depleted vegetation (Carlson and Kingston, 2014; Blumenthal et al., 2016). Given the size difference between *D. africanus* and *M. marymuunguae*, variation in body mass-related digestive physiologies and metabolic processes could have contributed to these $\delta^{13}\text{C}_{\text{enamel}}$ results (Passey et al., 2005; Tejada-Lara et al., 2018; Cerling et al., 2021).

The $\delta^{18}\text{O}_{\text{enamel}}$ values of *M. marymuunguae* are enriched relative to most other herbivores at Buluk, including *D. africanus*, suggesting that this species was less water-dependent and received a larger portion of its water from dietary vegetation. These higher $\delta^{18}\text{O}_{\text{enamel}}$ values could also be attributed to consuming foods enriched in $\delta^{18}\text{O}$,

such as fruits from higher in the woody canopy or a large proportion of leafy browse (Carter and Bradbury, 2016; Roberts et al., 2017). Other species of large-bodied kubanochoerine suids from Early Miocene deposits on Rusinga Island (Garrett, 2016) and the Middle Miocene deposits on Maboko Island (Arney et al., 2022) exhibit a much lower $\delta^{18}\text{O}_{\text{enamel}}$ signal relative to other fauna than *M. marymuunguae* from Buluk. At both Rusinga and Maboko Islands, kubanochoerine suids exhibit $\delta^{18}\text{O}_{\text{enamel}}$ values that are more depleted than most other herbivore taxa (Garrett, 2016; Arney et al., 2022), which is ecologically similar to the depleted $\delta^{18}\text{O}_{\text{enamel}}$ values of the extant, water-dependent giant forest hog (*Hylochoerus meinertzhageni*) and the red river hog (*Potamochoerus porcus*) (Harris and Cerling, 2002; Nelson, 2013; Cerling et al., 2015; Martin et al., 2015; Lazagabaster et al., 2021). The contrasting enriched $\delta^{18}\text{O}_{\text{enamel}}$ values of *M. marymuunguae* suggest feeding and/or drinking behavior that is unlike these extant taxa and other fossil kubanochoerines from localities with closed forest elements in the local habitat.

Only one of the two tragulid species at Buluk, *Dorcatherium pigotti*, could be sampled in this study. While no specimens of the larger congeneric *D. chappuisi* from Buluk were available for sampling, these two species exhibit overlapping $\delta^{13}\text{C}_{\text{enamel}}$ and $\delta^{18}\text{O}_{\text{enamel}}$ values at the Early Miocene locality of Kalodirr (Butts, 2019; Green et al., 2022), but disparate carbon and oxygen values at the Middle Miocene site of Maboko (Arney et al., 2022). The $\delta^{13}\text{C}_{\text{enamel}}$ values of *D. pigotti* from Buluk are enriched (mean $\delta^{13}\text{C}_{\text{enamel}}$ value = $-10.7\text{\textperthousand}$) relative to the water chevrotain (*Hyemoschus aquaticus*), the only extant African tragulid species (mean $\delta^{13}\text{C}_{\text{enamel}}$ value = $-13.9\text{\textperthousand}$, Cerling et al., 2004). Extant *H. aquaticus* is a nocturnal, forest-dwelling herbivore that primarily consumes fallen fruits, but also occasionally consumes insects and carrion (Dubost, 1987; Gautier-Hion et al., 1980; Hart, 1986). *Dorcatherium pigotti* from Buluk, along with the majority of Miocene tragulids from East Africa and Eurasia, appears to have had a wider range of browsing diets outside of forested habitats than the modern *H. aquaticus* (Nelson, 2007; Aiglstorfer et al., 2014).

Early and Middle Miocene Intersite Comparisons

Stable carbon isotope data from herbivore enamel is available from relatively few East African

Miocene sites older than 9 Ma (Cerling et al., 1997; Arney et al., 2022; MacLatchy et al., 2023), yet the few published $\delta^{13}\text{C}_{\text{enamel}}$ datasets have contributed substantially to our understanding of herbivore dietary isotope ecology within C_3 -dominated habitats. The new $\delta^{13}\text{C}_{\text{enamel}}$ data from Buluk can be compared with data from Moroto (21 Ma), Maboko (~16 Ma), and Fort Ternan (13.7 Ma) to help fill a gap in what is known about East African dietary paleoecology across the early to Middle Miocene transition (16-15 Ma) (Table 2).

The bulk $\delta^{13}\text{C}_{\text{enamel}}$ values from Buluk are not significantly different from the Early Miocene site Moroto (Figure 4; Table 4). Moroto's paleoenvironment has been reconstructed as a woodland setting in which herbivores consumed primarily water-stressed C_3 vegetation and potentially some C_4 vegetation (MacLatchy et al., 2023). The lack of statistically significant differences between bulk $\delta^{13}\text{C}_{\text{enamel}}$ values from Buluk and Moroto suggests that the landscape at Buluk likely also included open woodland elements with water-stressed C_3 vegetation. Herbivores from Buluk, however, exhibit a narrower range of $\delta^{13}\text{C}_{\text{enamel}}$ values than those from Moroto, and there is no isotopic evidence for any closed canopy forest elements nor of minor C_4 (or CAM) dietary components, as indicated by the end members of the Moroto $\delta^{13}\text{C}_{\text{enamel}}$ distribution (MacLatchy et al., 2023). While bulk $\delta^{13}\text{C}_{\text{enamel}}$ distributions are influenced by the taxonomic sampling and overall sample size, the narrower range of the larger Buluk sample ($n=67$) compared to the broader range of the smaller Moroto samples ($n=25$) implies that the differences in $\delta^{13}\text{C}_{\text{enamel}}$ range are likely not an artifact of sampling strategy.

The $\delta^{13}\text{C}_{\text{enamel}}$ values from Buluk and from Moroto are significantly more enriched than the two Middle Miocene sites, Maboko and Fort Ternan (Figure 4; Table 4). Middle Miocene deposits at Maboko include multiple time-successive beds, which have been reconstructed as primarily open forest/woodland mosaics without the presence of C_4 biomass or water-stressed C_3 vegetation (Arney et al., 2022). Fort Ternan, despite a long history of paleoenvironmental debate (Shipman et al., 1981; Pickford, 1983a, 1983b; Shipman, 1986; Retallack et al., 1990; Cerling et al., 1991; Kappelman, 1991; Retallak, 1992; Dugas and Retallack, 1993; Cerling et al., 1997), has yielded stable carbon isotope data from soil carbonates and herbi-

vore enamel that indicates a relatively open canopy C_3 -dominated ecosystem without the presence of C_4 biomass (Cerling et al., 1991; Cerling et al., 1997). Comparisons of the bulk $\delta^{13}\text{C}_{\text{enamel}}$ distributions between these Middle Miocene sites and Buluk suggest that herbivores at Buluk foraged within more open-canopy, relatively drier habitats with greater proportions of water-stressed C_3 vegetation than at Maboko or Fort Ternan. While multiple paleoecological proxies have demonstrated temporal and spatial habitat heterogeneity across East African Early Miocene localities (Peppe et al., 2023), landscape variation across East Africa during the Middle Miocene is less well known, due in large part to the small number of known Middle Miocene fossil localities, and it is difficult to say whether the differences in $\delta^{13}\text{C}_{\text{enamel}}$ values reported here reflect any spatial and/or temporal trends across the Early-Middle Miocene transition.

A comparison of representative taxonomic groups (hyracoids, proboscideans, rhinocerotids, giraffoids, tragulids, suoids, and anthracotheres) reveals substantial differences in herbivore foraging behaviors between Early and Middle Miocene localities in Kenya (Figure 4). The $\delta^{13}\text{C}_{\text{enamel}}$ values of Buluk taxa are higher than their Middle Miocene counterparts.

Specifically, comparisons of species that occur at both Buluk and Maboko (the deinothere *P. hobleyi*, the tragulid *D. pigotti*, and the hyracoid *A. championi*) demonstrate dietary differences that likely reflect environmental differences between these two sites. While the gomphothere *P. macinnesi* also occurs at both Buluk and Maboko, the single sample from Buluk limits comparisons that can be made for this taxon, although this specimen is more enriched than any *P. macinnesi* specimen from Maboko. All *D. pigotti* and *A. championi* $\delta^{13}\text{C}_{\text{enamel}}$ values from Buluk are relatively enriched and do not overlap with the values of their conspecifics from Maboko (mean *D. pigotti* value is 2.1‰ higher; mean *A. championi* value is 2.0‰ higher). There is overlap among the $\delta^{13}\text{C}_{\text{enamel}}$ distributions of *P. hobleyi* specimens from Buluk and Maboko, but the mean $\delta^{13}\text{C}_{\text{enamel}}$ value of the Buluk specimens is relatively enriched. These results suggest that species co-occurring between Buluk and Maboko likely had flexible diets and consumed various proportions of dietary items (e.g., leaves, fruits, C_3 grasses) depending on the local environment.

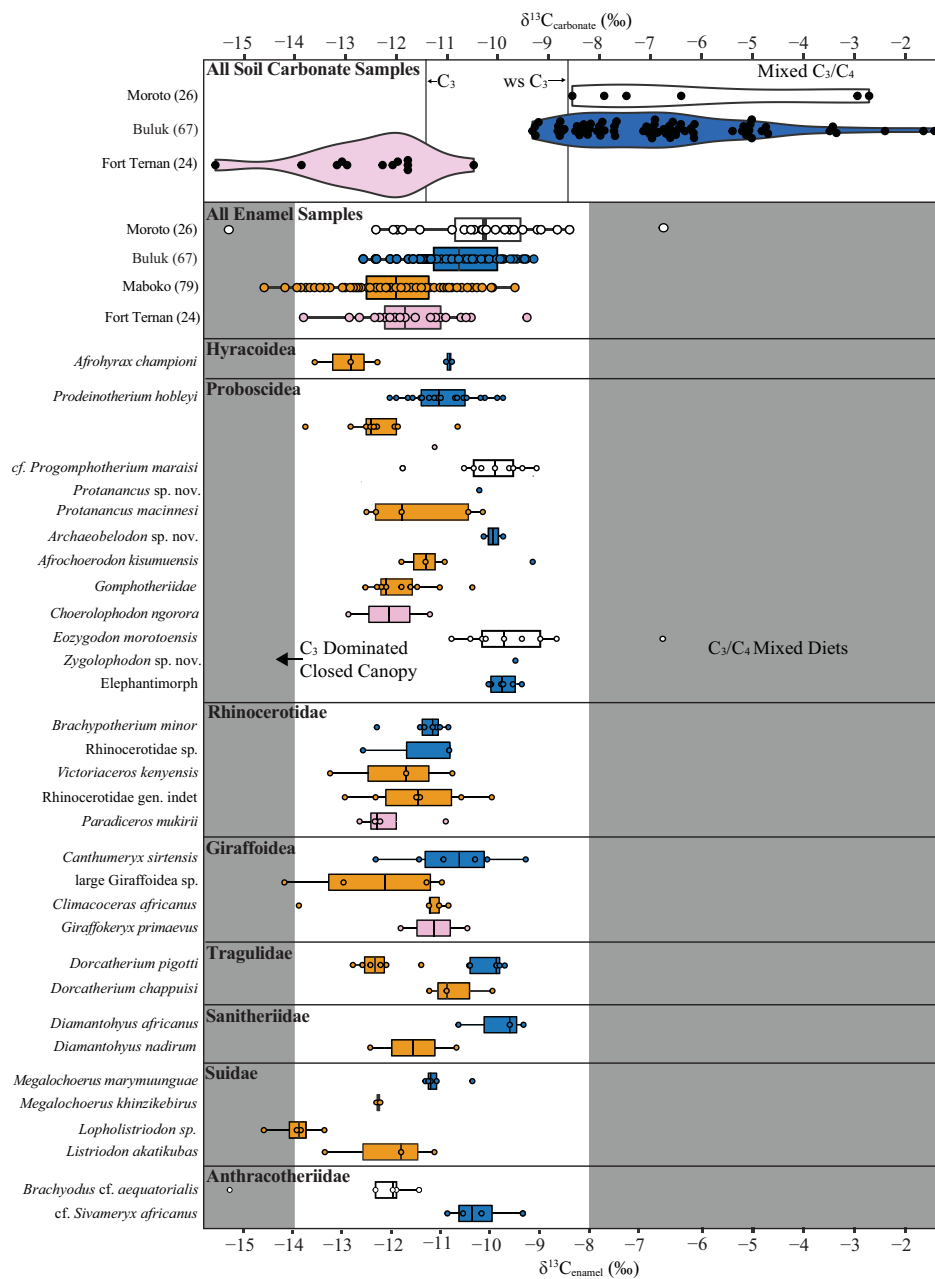


FIGURE 4. $\delta^{13}\text{C}_{\text{enamel}}$ value boxplots for Buluk (blue), Moroto (white), Maboko (orange), and Fort Ternan (pink) and violin plots of published $\delta^{13}\text{C}_{\text{carbonate}}$ values. The top panel labeled “All Soil Carbonate Samples” compares the violin plots of published $\delta^{13}\text{C}_{\text{carbonate}}$ values from Buluk (Peppe et al., 2023), Fort Ternan (Cerling et al., 1991), and Moroto (MacLatchy et al., 2023), which were corrected to a pre-Industrial $\delta^{13}\text{C}_{\text{atm}}$ value of -6.3‰. Vertical grey lines represent C₃ and water-stressed C₃ (ws C₃) endmembers estimated in Peppe et al., (2023) and corrected to a pre-Industrial $\delta^{13}\text{C}_{1750}$ value. Herbivore $\delta^{13}\text{C}_{\text{enamel}}$ values for Fort Ternan are from Cerling et al., (1997), $\delta^{13}\text{C}_{\text{enamel}}$ values for Maboko herbivores were taken from Arney et al., (2022), and $\delta^{13}\text{C}_{\text{enamel}}$ values for Moroto are extracted from MacLatchy et al., 2023. All carbon isotopic values are standardized to $\delta^{13}\text{C}_{1750}$ values. The panel of $\delta^{13}\text{C}_{\text{enamel}}$ values labeled “All Samples” compares boxplots of all herbivore $\delta^{13}\text{C}_{\text{enamel}}$ values from each locality. Bottom panels compare $\delta^{13}\text{C}_{\text{enamel}}$ values of taxonomic families between sites. The left grey panel designates $\delta^{13}\text{C}_{\text{enamel}}$ values falling within the range of closed canopy forest diets. The right grey panel indicates $\delta^{13}\text{C}_{\text{enamel}}$ values of mixed C_{3/C₄} diets.

TABLE 4. Significance levels from pair-wise Mann-Whitney U tests of bulk $\delta^{13}\text{C}_{\text{enamel}}$ values between sites. Results considered significant at $\alpha \leq 0.05$ are bolded.

Site (<i>n</i>)	Moroto	Buluk	Maboko	Fort Ternan
Moroto (26)	-			
Buluk (67)	0.07	-		
Maboko (79)	<0.001	<0.001	-	
Fort Ternan (21)	<0.001	<0.001	0.17	-

Additional comparisons at higher taxonomic levels broadly demonstrate greater $\delta^{13}\text{C}_{\text{enamel}}$ enrichment at Buluk and Moroto compared to Maboko and Fort Ternan (Figure 4). Among elephantimorphs, both *Eozygodon morotoensis* from Moroto (which has the highest $\delta^{13}\text{C}_{\text{enamel}}$ values of any elephantimorph in this sample) and the two taxa from Buluk demonstrate more enriched values than the Maboko and Fort Ternan specimens. Among suoids, *M. marymuunguae* and *D. africanus* from Buluk have higher $\delta^{13}\text{C}_{\text{enamel}}$ values than their congeners (*Megaloceroerus khinzikebirus* and *Diamantohyus nadirum*) from Maboko, indicating different dietary preferences and/or vegetation availability between these sites. The sole giraffoid from Buluk, *C. sirtensis*, exhibits slightly enriched $\delta^{13}\text{C}_{\text{enamel}}$ values relative to *Climacoceras africanus* from Maboko but overlaps with the large Giraffoidea sp. from Maboko and *Giraffokeryx primaevis* from Fort Ternan. Rhinocerotidae is the only taxonomic group that demonstrates considerable overlap in $\delta^{13}\text{C}_{\text{enamel}}$ values across Early and Middle Miocene sites. The extensive overlap between the rhinocerotid samples from Buluk, Maboko, and Fort Ternan suggests limited dietary variation among these species and possibly less flexible feeding ecology than other mammalian groups.

Of the taxonomic groups that overlap between Buluk and Moroto, only the anthracothere show differences in $\delta^{13}\text{C}_{\text{enamel}}$ values. The Moroto anthracothere, *Brachyodus cf. aequatorialis*, has depleted $\delta^{13}\text{C}_{\text{enamel}}$ values relative to cf. *Sivameryx africanus* from Buluk. One interpretation of these results is that *B. cf. aequatorialis* at Moroto inhabited wetter, more densely vegetated habitats relative to cf. *S. africanus* at Buluk. This may be more indicative of differences in the behavior and biology of these taxa, which differ in size and dental morphology, rather than environmental differ-

ences between these sites. The low $\delta^{18}\text{O}_{\text{enamel}}$ values of *B. cf. aequatorialis* relative to other Moroto herbivore $\delta^{18}\text{O}_{\text{enamel}}$ values (Appendix 5; see also fig. S12 of MacLatchy et al., 2023) support the idea that this taxon might have been more water dependent than cf. *S. africanus* at Buluk. *Brachyodus* and *Sivameryx* have been suggested to be a hydrophilic taxon based on depositional and taphonomic settings at North African and some East African Miocene localities (Pickford, 1983; Holroyd et al., 2010; Miller et al., 2014), although cranial remains of *Sivameryx africanus* from the Early Miocene locality of Kalodirr have cast doubt on the proposal that this species was semi-aquatic (Rowan et al., 2015).

Prior to the publication of stable carbon isotope data from the Early Miocene in East Africa, variation in ^{13}C among plants in C_3 -dominated ecosystems was presumed to be too limited for dietary inference or palaeoecological reconstruction (MacLatchy et al., 2023). Here, however, the collective ranges of dietary carbon signals from herbivore guilds at Moroto, Buluk, Maboko, and Fort Ternan document shifting foraging strategies across the Early and Middle Miocene. While caution should be used when using herbivore $\delta^{13}\text{C}_{\text{enamel}}$ values for paleoenvironmental comparisons, especially when inferring differences in woody cover (Robinson et al., 2021), the considerable C_3 -dominated dietary heterogeneity documented in these intersite results is consistent with independent lines of palaeoecological evidence for variable habitat cover and vegetation at these Early and Middle Miocene sites (e.g., Lukens et al., 2021; MacLatchy et al., 2023; Peppe et al., 2023).

East African Miocene Environments and Catarrhine Evolution

Early models of the environmental context for early catarrhine evolution emphasized pervasive complex canopy cover across eastern Africa during the Early Miocene, eventually giving way to more fragmented woodlands in the late Early Miocene and the Middle Miocene (e.g., Andrews and Van Couvering, 1975; Andrews and Kelley, 2007; Couvreur et al., 2008). A more recent body of soil carbonate and plant wax isotopic datasets from multiple Early Miocene sites has indicated the presence of more eclectic habitats across this region, ranging from closed canopy forests to wooded grasslands with arid conditions that could support substantial C_4 plant components (Lukens et al., 2017a; Liutkus-Pierce et al., 2018;

MacLatchy et al., 2023; Peppe et al., 2023). Buluk, along with the Karungu, Moroto, and Napak have been identified as some of the sites with C₄ isotopic biomass signatures from pedogenic carbonates, and the presence of PACMAD (Panicoideae, Arundinoideae, Chloridoideae, Micrairoideae, Aristioideae, Danthonoideae) phytoliths at six Early Miocene sites suggests the presence of potentially C₄ grasses on the landscape (Peppe et al., 2023) (Figure 5A, B).

In contrast, evidence from herbivore $\delta^{13}\text{C}_{\text{enamel}}$ values reveals the persistence of pure C₃ or C₃-dominated diets during this time period (Figure 5C). The C₃-dominated diets of herbivores at Buluk, as well as Moroto, contrast with the considerable C₄ signal derived from paleosol carbonates, suggesting that these C₄ plants were not consumed in sufficient quantities to be reflected in the $\delta^{13}\text{C}_{\text{enamel}}$ values of the taxa sampled here. The nature of the opportunistic sampling strategy allows for the possibility that one or more of the taxa that were not sampled may have consumed some amount of C₄ vegetation. That is, sampling biases from the availability of dental remains among both the Buluk and Moroto collections could be underestimating the total range of herbivore $\delta^{13}\text{C}_{\text{enamel}}$ values, particularly at the higher end of the range.

Differences in temporal scale between isotopic proxies may also help explain the discrepancy between paleosol and herbivore enamel isotope results. Enamel isotopes reflect vegetation consumed over a shorter duration of time (months to years), while soil isotopes reflect a local vegetation signal that is averaged over thousands of years (Koch, 1998). The mobility of herbivores also suggests that $\delta^{13}\text{C}_{\text{enamel}}$ values reflect vegetation from a wider geographic area than paleosol carbonates, and the discrepancy between the two proxies is possible if herbivores foraged on C₃ resources in more distant areas from where carbonate nodules were collected (Du et al., 2019). As a result, enamel isotopes likely capture a short-term phase of vegetation and a wider area of foraging where C₄ plants were not abundant or utilized, while carbonates capture long-term, seasonally drier intervals in a more localized area that would have favored spikes in C₄ plants and the formation of soil carbonates (Peppe et al., 2023). In a mature river system, like the one interpreted for Buluk, it is also possible that the pedogenic carbonates might not have recorded a C₃ endmember signal since

the time of carbonate formation exceeds that of the channel position with its C₃ vegetation (Levin et al., 2004). In other words, pedogenic carbonate forming beneath a riverbank and its riparian woodland would have migrated further distally or eroded by a change in the river channel position. Additionally, it is also possible that the presence of diagenesis in enamel and/or pedogenic carbonate samples could be influencing this incongruity.

Beginning in the late Oligocene and Early Miocene, tectonic activity in eastern Africa (e.g., rift valley formation, volcanism, uplift of the East African Plateau) is believed to have been a force shaping regional climatic variation and local scale habitat heterogeneity across eastern Africa (Sepulchre et al., 2006; Wighura et al., 2015; Linder, 2017; Peppe et al., 2023; Munday et al., 2023). The accumulation of multi-proxy paleoenvironmental data documenting extensive habitat heterogeneity across East Africa during the Early and Middle Miocene (Michel et al., 2014, 2020; Driese et al., 2016; Lukens et al., 2017; Liutkus-Pierce et al., 2019; Baumgartner and Peppe, 2021; MacLatchy et al., 2023; Peppe et al., 2023) has complicated previous adaptive models of catarrhine evolution that posited the emergence of hominoid diet and locomotion within widespread forest environments (e.g., Napier, 1967; Temerin and Cant, 1983; Hunt, 2016). Concomitant with this emerging picture of eastern African habitat heterogeneity is a growing body of evidence for a wide array of locomotor and dietary diversity among Early and Middle Miocene catarrhines (e.g., Wuthrich et al. 2019; Nishimura et al., 2022; MacLatchy et al., 2023). The Buluk herbivore enamel isotope results presented here provide additional evidence documenting the presence of open canopy woodland habitats inhabited by Early Miocene catarrhines. Additionally, the extent of niche separation among Buluk herbivores, as well as the separation between conspecific and congeneric taxa at Buluk and Maboko demonstrates that Early and Middle Miocene herbivores utilized complex and variable dietary behaviors on this heterogeneous East African landscape, and the primates may have done the same.

CONCLUSIONS

Buluk is a terminal Early Miocene locality that preserves a rich mammalian fauna including a diversity of fossil catarrhines. Herbivore $\delta^{13}\text{C}_{\text{enamel}}$ values indicate that Buluk mammals lived and foraged in an arid, C₃-dominated, open canopy wood-

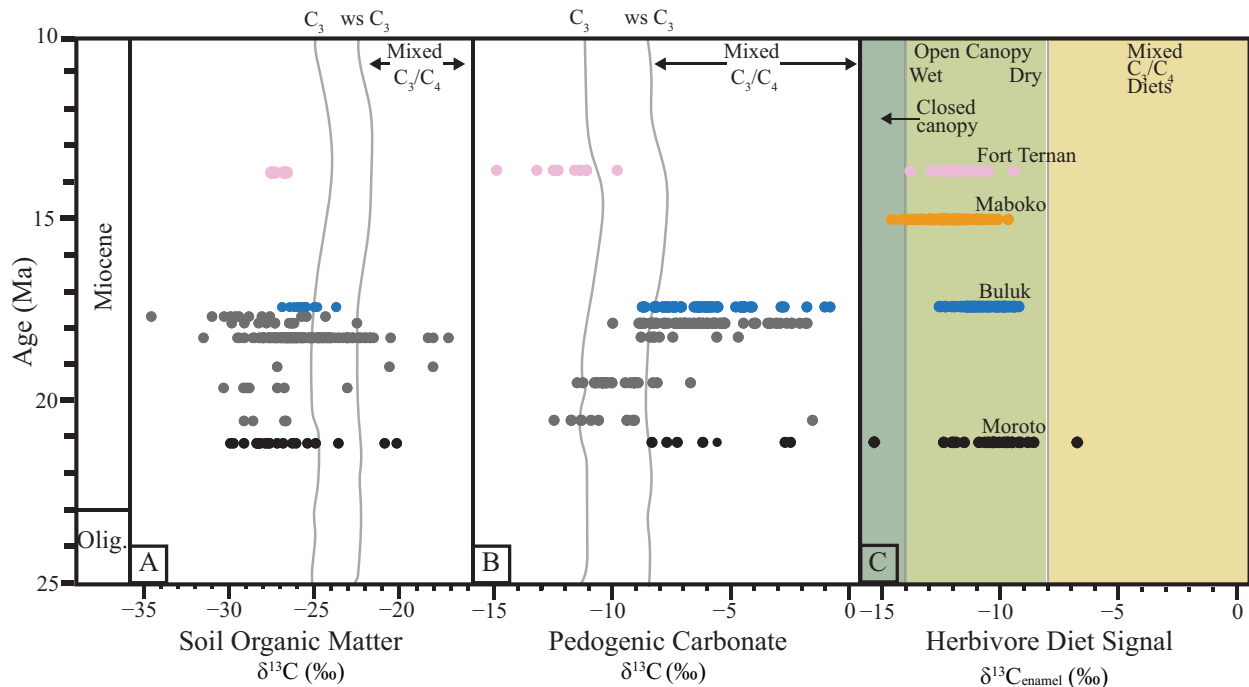


FIGURE 5. Long-term record of soil organic matter, pedogenic carbonate, and enamel stable carbon isotopes from the late Oligocene to late Miocene. The left and middle panels are published soil organic (A) and pedogenic carbonate (B) carbon isotopic values from early Miocene localities (Peppe et al., 2023) and Fort Ternan (Cerling et al., 1991). Vertical grey lines indicate C_3 and water-stressed C_3 (ws C_3) endmember $\delta^{13}C$ values calculated and standardized for atmospheric CO_2 $\delta^{13}C$. Data from Buluk (blue), Moroto (black), and Fort Ternan (pink) are highlighted. The right panel shows Buluk and published herbivore enamel $\delta^{13}C$ values (C) from Moroto (MacLatchy et al., 2023), Maboko (Arney et al., 2022), and Fort Ternan (Cerling et al., 1997). Maboko data is highlighted in orange. From left to right, straight, vertical lines represent closed canopy habitats and mixed C_3/C_4 endmember enamel $\delta^{13}C$ values. Panels A and B are modified from “Oldest evidence of abundant C_4 grasses and habitat heterogeneity in eastern Africa” by Peppe et al., 2023, Science, 380(6641), page 176. Panels A and B of the image are not published under the terms of the CC-BY license of this article. For permission to reuse, please see Peppe et al. (2023).

land environment, as indicated by the tightly constrained range of $\delta^{13}C_{\text{enamel}}$ values (-12.7‰ to -9.4‰). Herbivores at Buluk had C_3 -dominated diets with no evidence for consumption of C_4 resources, despite their presence on the landscape (Peppe et al., 2023). Taxa with the lowest $\delta^{13}C_{\text{enamel}}$ values include rhinocerotids and deinotheres, while the highest values are among elephantimorph proboscideans and sanitheriid suoids. The relatively high $\delta^{18}O_{\text{enamel}}$ range among Buluk herbivores may reflect extensive fluctuation in $\delta^{18}O$ values, which may be a consequence of precipitation seasonality, multiple local water sources, or sampling several water sources during seasonal migration. Results of serial oxygen isotopic analyses of herbivore teeth would test for seasonality (e.g., Green et al., 2022), while comparisons of Buluk herbivore strontium isotopic ratios with bioavailable

$^{87}Sr/^{86}Sr$ could potentially test for herbivore mobility (Janzen et al., 2020).

Comparisons with $\delta^{13}C_{\text{enamel}}$ data from fauna at the Early Miocene site Moroto and the Middle Miocene sites Maboko and Fort Ternan indicate a shift from more enriched signals in the Early Miocene to more depleted ones in the Middle Miocene. The similarity between the Moroto and Buluk $\delta^{13}C_{\text{enamel}}$ value distributions suggests the dominance of water-stressed C_3 vegetation at these sites, although the broader range of values from Moroto implies greater habitat variability, including the presence of some closed-canopy elements and the consumption of limited C_4 grasses, which are not documented at Buluk. Stable carbon isotope data have previously affirmed the similarity in paleoenvironments between the Middle Miocene sites of Maboko and Fort Ternan (Arney et al.,

2022). Compared to the herbivores from these Middle Miocene sites, herbivores from Buluk foraged in a more open canopy, water-stressed ecosystem. Shared taxa between Buluk and Maboko (*P. hobleyi*, *A. championi*, and *D. pigotti*) have $\delta^{13}\text{C}_{\text{enamel}}$ values that reflect consistently ^{13}C enriched diets at Buluk. These findings are consistent with recent reconstructions of a subhumid woodland environment at Buluk based on geochemical data (Lukens et al., 2017b, 2021) and contribute to the growing body of evidence for environmental and dietary heterogeneity across space and time in the East African Miocene (Peppe et al., 2023).

Despite the growing body of geochemical and palaeobotanical evidence for C_4 biomass in eastern Africa during the Early and Middle Miocene (Kingston et al., 1994; Morgan et al., 1994; Lukens et al., 2017a; MacLatchy et al., 2023; Peppe et al., 2023), $\delta^{13}\text{C}_{\text{enamel}}$ data from Buluk provides no evidence of a C_4 dietary signal among mammalian herbivores. The absence of a C_4 component in herbivore diets could reflect the differences in temporal scale captured by stable isotopes from tooth enamel and pedogenic carbonates. It may be that the C_4 biomass present at Buluk during the lifespan of herbivores sampled was in low enough proportion that it was not a preferred dietary item for herbivorous mammals, or they consumed this material in quantities too low to impact bulk enamel $\delta^{13}\text{C}$ values.

Future research could expand the understanding of individual dietary variability and dietary

variation across herbivore guilds in the C_3 -dominated ecosystem at Buluk by applying additional dietary proxies (e.g., mesowear, microwear) and serial isotopic sampling of herbivore molars. To further assess shifting diets and environments across the Early-Middle Miocene transition, more targeted sampling of additional Buluk taxa that persisted into the Middle Miocene (e.g., *Dorcatherium chappuisi*, *Lopholistriondon pickfordi*, cf. *Kenyasus rusinensis*, and cf. *Propaleoryx nyanzae*; see Table 1) should be prioritized if additional dental specimens are recovered.

ACKNOWLEDGEMENTS

Funding for this work was provided by the Leakey Foundation, the Turkana Basin Institute, National Geographic, and the Foothill De-Anza Foundation. We would like to thank the Kenyan National Commission for Science, Technology, and Innovation (NACOSTI) for permission to conduct this research. We would also like to thank the Department of Earth Sciences at the National Museums of Kenya and the Turkana Basin Institute for access to fossil specimens and permission for sampling. Thanks to B. Sanders for identifying the proboscideans fossils from Buluk and to J. Kingston, N. Levin, and L. MacLatchy for guidance and feedback during the project development phase. We are grateful for comments from K. Uno and one anonymous reviewer. Finally, many thanks to the Buluk field crew without whom this work would not have been possible.

REFERENCES

- Aiglstorfer, M., Bocherens, H., and Böhme, M. 2014. Large mammal ecology in the late middle Miocene gratkorn locality (Austria). *Palaeobiodiversity and Palaeoenvironments*, 94:189–213. <https://doi.org/10.1007/s12549-013-0145-5>
- Andrews, P. and Kelley, J. 2007. Middle Miocene dispersals of apes. *Folia primatologica*, 78:328–343. <https://doi.org/10.1159/000105148>
- Andrews, P. and Martin, L. 1991. Hominoid dietary evolution. *Philosophical Transactions of the Royal Society*, 334:199–209. <https://doi.org/10.1098/rstb.1991.0109>
- Andrews, P. and VanCouvering, J.A. 1975. Palaeoenvironments in the East African Miocene, p. 62–103. In Szalay, F.S. (ed.), *Approaches to Primate Paleobiology, Contributions to Primateology, Volume 5*. Karger.
- Andrews, P., Lord, J.M., and Nesbit Evans, E.M. 1979. Patterns of ecological diversity in fossil and modern mammalian faunas. *Biological Journal of the Linnean Society*, 11:177–205. <https://doi.org/10.1111/j.1095-8312.1979.tb00034.x>

- Andrews, P., Meyer, G.E., Pilbeam, D.R., Van Couvering, J.A., and Van Couvering, J.A.H. 1981. The Miocene fossil beds of Maboko Island, Kenya: Geology, age, taphonomy and palaeontology. *Journal of Human Evolution*, 10:35–48.
[https://doi.org/10.1016/S0047-2484\(81\)80024-3](https://doi.org/10.1016/S0047-2484(81)80024-3)
- Arney, I., Benefit, B.R., McCrossin, M.L., MacLatcy, L., and Kingston, J.D. 2022. Herbivore isotopic dietary ecology of the middle Miocene Maboko Formation, Kenya. *Palaeogeography, Palaeoclimatology, Palaeoecology*, 601:111061.
<https://doi.org/10.1016/j.palaeo.2022.111061>
- Baumgartner, A. and Peppe, D.J. 2021. Paleoenvironmental changes in the Hiwegi Formation (lower Miocene) of Rusinga Island, Lake Victoria, Kenya. *Palaeogeography, Palaeoclimatology, Palaeoecology*, 574:110458.
<https://doi.org/10.1016/j.palaeo.2021.110458>
- Benefit, B. 1999. *Victoriapithecus*: the key to Old World monkey and catarrhine origins. *Evolutionary Anthropology*, 7:155–174.
[https://doi.org/10.1002/\(SICI\)1520-6505\(1999\)7:5<155::AID-EVAN2>3.0.CO;2-D](https://doi.org/10.1002/(SICI)1520-6505(1999)7:5<155::AID-EVAN2>3.0.CO;2-D)
- Blumenthal, S.A., Rothman, J.M., Chritz, K.L., and Cerling, T.E. 2016. Stable isotopic variation in tropical forest plants for applications in primatology. *Journal of Primatology*, 78:1041–1054.
<https://doi.org/10.1002/ajp.22488>
- Blumenthal, S.A., Levin, N.E., Brown, F.H., Brugal, J.-P., Chritz, K.L., Harris, J.M., Jehle, G.E., and Cerling, T.E. 2017. Aridity and hominin environments. *Proceedings from the National Academy of Science*, 114:7331–7336.
<https://doi.org/10.1073/pnas.1700597114>
- Bocherens, H., Koch, P.L., Mariotti, A., Geraads, D., and Jaeger, J.J. 1996. Isotopic Biogeochemistry (^{13}C , ^{18}O) of mammalian enamel from African Pleistocene Hominid Sites. *Palaios*, 11:306–318.
<https://doi.org/10.2307/3515241>
- Bonnefille, R. 1984. Cenozoic vegetation and environments of early hominids in East Africa. *The Evolution of the East Asian Environment*, 2:579–612.
- Bonnefille, R. 2010. Cenozoic vegetation, climate changes and hominid evolution in tropical Africa. *Global and Planetary Change*, 72:390–411.
<https://doi.org/10.1016/J.GLOPLACHA.2010.01.015>
- Bryant, D.J. and Froelich, P.N. 1995. A model of oxygen isotope fractionation in body water of large mammals. *Geochimica et Cosmochimica Acta*, 59:4523–4537.
- Butts, C.F.R. 2019. Paleoenvironmental Reconstruction of Kalodirr and Moruorot, Kenya using Stable Carbon Isotopes. Unpublished Masters Thesis, University of Calgary, Calgary, AB, Canada.
- Carlson, B.A. and Kingston, J.D. 2014. Chimpanzee isotopic ecology: A closed canopy C_3 template for hominin dietary reconstruction. *Journal of Human Evolution*, 76:107–115.
<https://doi.org/10.1016/J.JHEVOL.2014.06.001>
- Carter, M.L. and Bradbury, M.W. 2016. Oxygen isotope ratios in primate bone carbonate reflect amount of leaves and vertical stratification in the diet. *American Journal of Primatology*, 78:1086–1097.
<https://doi.org/10.1002/AJP.22432>
- Cerling, T.E. and Harris, J.M. 1999. Carbon isotope fractionation between diet and bioapatite in ungulate mammals and implications for ecological and paleoecological studies. *Oecologia*, 120:347–363.
<https://doi.org/10.1007/s004420050868>
- Cerling, T.E., Quade, J., Ambrose, S.H., and Sikes, N.E. 1991. Fossil soils, grasses, and carbon isotopes from Fort Ternan, Kenya: grassland or woodland? *Journal of Human Evolution*, 21:295–306.
[https://doi.org/10.1016/0047-2484\(91\)90110-H](https://doi.org/10.1016/0047-2484(91)90110-H)
- Cerling, T.E., Harris, J.M., Ambrose, S.H., Leakey, M.G., and Solounias, N. 1997. Dietary and environmental reconstruction with stable isotope analyses of herbivore tooth enamel from the Miocene locality of Fort Ternan, Kenya. *Journal of Human Evolution*, 33:635–650.
<https://doi.org/10.1006/jhev.1997.0151>
- Cerling, T.E., Harris, J.M., and Leakey, M.G. 1999. Browsing and grazing in elephants: the isotope record of modern and fossil proboscideans. *Oecologia*, 120:364–374.
<https://doi.org/10.1007/s004420050869>

- Cerling, T.E., Harris, J.M., Leakey, M.G. and Mudida, N. 2003a. Stable isotope ecology of northern Kenya, with emphasis on the Turkana Basin, p. 583–603. In Leakey, M.G., Harris J.M., (eds.), Lothagam: the dawn of humanity in eastern Africa. New York: Columbia University Press.
- Cerling, T.E., Harris, J.M. and Leakey, M.G. 2003b. Isotope Paleoecology of the Nawata and Nachukui Formations at Lothagam, Turkana Basin, Kenya, p. 605–624. In Leakey, M.G. and Harris J.M., (eds.), Lothagam: The Dawn of Humanity in Eastern Africa.
- Cerling, T.E., Hart, J.A., and Hart, T.B. 2004. Stable isotope ecology in the Ituri Forest. *Oecologia*, 138:5–12.
<https://doi.org/10.1007/s00442-003-1375-4>
- Cerling, T.E., Andanje, S.A., Blumenthal, S.A., Brown, F.H., Chritz, K.L., Harris, J.M., Hart, J.A., Kirera, F.M., Kaleme, P., Leakey, L.N., Leakey, M.G., Levin, N.E., Manthi, F.K., Passey, B.H., and Uno, K.T. 2015. Dietary changes of large herbivores in the Turkana Basin, Kenya from 4 to 1 Ma. *Proceedings from the National Academy of Science*, 112:11467–11472.
<https://doi.org/10.1073/pnas.1513075112>
- Cerling, T.E., Bernasconi, S.M., Hofstetter, L.S., Jaggi, M., Wyss, F., Rudolf von Rohr, C., and Clauss, M. 2021. CH₄/CO₂ Ratios and carbon isotope enrichment between diet and breath in herbivorous mammals. *Frontiers in Ecology and Evolution*, 9:638568.
<https://doi.org/10.3389/fevo.2021.638568>
- Clementz, M.T., Holroyd, P.A., and Koch, P.L. 2008. Identifying aquatic habits of herbivorous mammals through stable isotope analysis. *Palaios*, 23:574–585.
<https://doi.org/10.2110/palo.2007.p07-054r>
- Cote, S., Kingston, J., Deino, A., Winkler, A., Kityo, R., and MacLatchy, L. 2018. Evidence for rapid faunal change in the early Miocene of East Africa based on revised biostratigraphic and radiometric dating of Bukwa, Uganda. *Journal of Human Evolution*, 116:95–107.
<https://doi.org/10.1016/j.jhevol.2017.12.001>
- Couvreur, T.L.P., Chatrou, L.W., Sosef, M.S.M., and Richardson, J.E. 2008. Molecular phylogenetics reveal multiple tertiary vicariance origins of the African rain forest trees. *BMC Biology*, 6:54.
<https://doi.org/10.1186/1741-7007-6-54>
- Dansgaard, W. 1964. Stable isotopes in precipitation. *Tellus*, 16:436–468.
<https://doi.org/10.3402/tellusa.v16i4.8993>
- Davis, S.J.M. 1980. A note on the dental and skeletal ontogeny of *Gazella*. *Israel Journal of Zoology*, 29:129–134.
- Driese, S.G., Peppe, D.J., Beverly, E.J., DiPietro, L.M., Arellano, L.N., and Lehmann, T. 2016. Paleosols and paleoenvironments of the early Miocene deposits near Karungu, Lake Victoria, Kenya. *Palaeogeography, Palaeoclimatology, Palaeoecology*, 443:167–182.
<https://doi.org/10.1016/j.palaeo.2015.11.030>
- Du, A., Rowan, J., Lazagabaster, I.A., Behrensmeyer, A.K., and Robinson, J.R. 2019. Stable carbon isotopes from paleosol carbonate and herbivore enamel document differing paleovegetation signals in the eastern African Plio-Pleistocene. *Review of Palaeobotany and Palynology*, 261:41–52.
<https://doi.org/10.1016/j.revpalbo.2018.11.003>
- Dugas, D.P. and Retallack, G.J. 1993. Middle Miocene fossil grasses from Fort Ternan. *Journal of Paleontology*, 67:113–128.
<https://doi.org/10.1017/S0022336000021223>
- Ehleringer, J.R., Field, C.B., Lin, Z., and Kuo, C. 1986. Leaf carbon isotope and mineral composition in subtropical plants along an irradiance cline. *Oecologia*, 70:520–526.
<https://doi.org/10.1007/BF00379898>
- Fannin, L.D. and McGraw, W.S. 2020. Does oxygen stable isotope composition in primates vary as a function of vertical stratification or folivorous behaviour? *Folia Primatologica*, 91:219–227.
<https://doi.org/10.1159/000502417>
- Feakins, S.J., Levin, N.E., Liddy, H.M., Sieracki, A., Eglinton, T.I., and Bonneville, R. 2013. Northeast African vegetation change over 12 m.y. *Geology*, 41:295–298.
<https://doi.org/10.1130/G33845.1>
- Feibel, C.S. and Brown, F.H. 1991. Age of the primate-bearing deposits on Maboko Island, Kenya. *Journal of Human Evolution*, 21:221–225.
[https://doi.org/10.1016/0047-2484\(91\)90063-2](https://doi.org/10.1016/0047-2484(91)90063-2)

- Francey, R.J., Allison, C.E., Etheridge, D.M., Trudinger, C.M., Enting, I.G., Leuenberger, M., Langenfelds, R.L., Michel, E., and Steele, L.P. 1999. A 1000-year high precision record of $\delta^{13}\text{C}$ in atmospheric CO_2 . *Tellus*, 51:170–193.
<https://doi.org/10.1034/j.1600-0889.1999.t01-1-00005.x>
- Fricke, H.C. and O'Neil, J.R. 1996. Inter-and intra-tooth variation in the oxygen isotope composition of mammalian tooth enamel phosphate: implications for palaeoclimatological and palaeobiological research. *Palaeogeography, Palaeoclimatology, Palaeoecology*, 126:91–99.
[https://doi.org/10.1016/S0031-0182\(96\)00072-7](https://doi.org/10.1016/S0031-0182(96)00072-7)
- Fricke, J.R., Clyde, W.C., and O'Neil, J.R. 1998. Intra-tooth variations in $\delta^{18}\text{O}$ (PO_4) of 839 mammalian tooth enamel as a record of seasonal variations in continental climate variables. *Geochimica et Cosmochimica Acta*, 62:1839–1850.
[https://doi.org/10.1016/S0016-7037\(98\)00114-8](https://doi.org/10.1016/S0016-7037(98)00114-8)
- Garrett, N. 2016. Stable isotope paleoenvironmental reconstructions of the Late Pleistocene and Early Miocene sites on Rusinga and Mfangano Islands, Lake Victoria, Kenya. Unpublished Ph.D. Dissertation, University of Minnesota, Minneapolis, MN, USA.
- Gautier-Hion, A., Emmons, L.H., and Dubost, G. 1980. A comparison of the diets of three major groups of primary consumers of Gabon (primates, squirrels and ruminants). *Oecologia*, 45:182–189.
<https://doi.org/10.1007/BF00346458>
- Geraads, D. and Miller, E. 2013. *Brachypotherium minor* n. sp., and other Rhinocerotidae from the Early Miocene of Buluk, Northern Kenya. *Geodiversitas*, 35:359–375.
<https://doi.org/10.5252/g2013n2a5>
- Green, D.R., Olack, G., and Colman, A.S. 2018. Determinants of blood water $\delta^{18}\text{O}$ variation in a population of experimental sheep: Implications for paleoclimate reconstruction. *Chemical Geology*, 485:32–43.
<https://doi.org/10.1016/J.CHEMGEO.2018.03.034>
- Green, D.R., Ávila, J.N., Cote, S., Dirks, W., Lee, D., Poulsen, C.J., Williams, I.S., and Smith, T.M. 2022. Fine-scaled climate variation in equatorial Africa revealed by modern and fossil primate teeth. *Proceedings of the National Academy of Sciences*, 119:e2123366119.
<https://doi.org/10.1073/pnas.2123366119>
- Grossman, A. 2008. Ecological and morphological diversity in catarrhine primates from the Miocene of Africa. Unpublished Ph.D. Dissertation, Stony Brook University, Stony Brook, New York, USA.
- Hall, A.S. and Cote, S. 2021. Ruminant mesowear reveals consistently browse-dominated diets throughout the early and middle Miocene of eastern Africa. *Palaeogeography, Palaeoclimatology, Palaeoecology*, 567:110253.
<https://doi.org/10.1016/j.palaeo.2021.110253>
- Harris, J.M. and Cerling, T.E. 2002. Dietary adaptations of extant and Neogene African suids. *Journal of Zoology*, 256:45–54.
<https://doi.org/10.1017/S0952836902000067>
- Harris, J.M. and Watkins, R. 1974. New early Miocene vertebrate locality near Lake Rudolf, Kenya. *Nature*, 252:576–577.
<https://doi.org/10.1038/252576a0>
- Hart, J. 1986. Comparative dietary ecology of a community of frugivorous forest ungulates in Zaire (ruminants, feeding habits, rainforest). PhD Dissertation, Michigan State University, East Lansing, MI, USA.
- Heaton, T.H.E. 1999. Spatial, species, and temporal variations in the $^{13}\text{C}/^{12}\text{C}$ ratios of C_3 plants: implications for paleodiet studies. *Journal of Archaeological Sciences*, 26:637–649. <https://doi.org/10.1006/jasc.1998.0381>
- Higgins, P. and MacFadden, B.J. 2004. “Amount Effect” recorded in oxygen isotopes of Late Glacial horse (*Equus*) and bison (*Bison*) teeth from the Sonoran and Chihuahuan deserts, southwestern United States. *Palaeogeography, Palaeoclimatology, Palaeoecology*, 206:337–353. <https://doi.org/10.1016/j.palaeo.2004.01.011>
- Hillman-Smith, A.K.K., Anderson, J.L., Hall-Martin, A.J., and Selaladi, D.J.P. 1986. Age estimation of the White rhinoceros (*Ceratotherium simum*). *Journal of Zoology*, 210:355–379.
<https://doi.org/10.1111/j.1469-7998.1986.tb03639.x>

- Holroyd, P.A., Lihoreau, F., Gunnell, G.F., and Miller, E. 2010. Anthracotheriidae, p. 851–859. In Werdelin, L. and Sanders, W. (eds.), *Cenozoic Mammals of Africa*. University of California Press, Berkeley, California.
- Hunt, K.D. 2016. Why are there apes? Evidence for the co-evolution of ape and monkey ecomorphology. *Journal of Anatomy*, 228:630–685.
<https://doi.org/10.1111/joa.12454>
- Hurford, A.J. and Watkins, R.T. 1987. Fission-track age of the tuffs of the Buluk member, Bakate formation, Northern Kenya: A suitable fission-track age standard. *Chemical Geology: Isotope Geoscience section*, 66:209–216.
[https://doi.org/10.1016/0168-9622\(87\)90042-X](https://doi.org/10.1016/0168-9622(87)90042-X)
- Janzen, A., Bataille, C., Copeland, S.R., Quinn, R.L., Ambrose, S.H., Reed, D., Hamilton, M., Grimes, V., Richards, M.P., le Roux, P., and Roberts, P. 2020. Spatial variation in bioavailable strontium isotope ratios ($^{87}\text{Sr}/^{86}\text{Sr}$) in Kenya and northern Tanzania: Implications for ecology, paleoanthropology, and archaeology. *Palaeogeography, Palaeoclimatology, Palaeoecology*, 560: 109957.
<https://doi.org/10.1016/j.palaeo.2020.109957>
- Kappleman, J. 1991. The paleoenvironment of *Kenyapithecus* at Fort Ternan. *Journal of Human Evolution*, 20:95–129.
[https://doi.org/10.1016/0047-2484\(91\)90053-X](https://doi.org/10.1016/0047-2484(91)90053-X)
- Kingston, J.D. and Harrison, T. 2007. Isotopic dietary reconstructions of Pliocene herbivores at Laetoli: Implications for early hominin paleoecology. *Palaeogeography, Palaeoclimatology, Palaeoecology*, 243:272–306.
<https://doi.org/10.1016/j.palaeo.2006.08.002>
- Kingston, J.D., Hill, A., and Marino, B.D. 1994. Isotopic evidence for Neogene hominid paleoenvironments in the Kenyan Rift Valley. *Science*, 264:955–959.
<https://doi.org/10.1126/science.264.5161.955>
- Koch, P.L. 1998. Isotopic reconstruction of past continental environments. *Annual Review of Earth and Planetary Sciences*, 26:573–613.
<https://doi.org/10.1146/annurev.earth.26.1.573>
- Kohn, M.J. 1996. Predicting animal $\delta^{18}\text{O}$: Accounting for diet and physiological adaptation. *Geochimica et Cosmochimica Acta*, 60:4811–4829.
[https://doi.org/10.1016/S0016-7037\(96\)00240-2](https://doi.org/10.1016/S0016-7037(96)00240-2)
- Kohn, M.J. 2010. Carbon isotope compositions of terrestrial C3 plants as indicators of paleoecology and paleoclimate. *Proceedings of the National Academy of Sciences*, 46:19691–19695.
<https://doi.org/10.1073/pnas.1004933107>
- Kohn M.J. and Law, J.M. 2006. Stable isotope chemistry of fossil bone as a new paleoclimate indicator. *Geochimica et Cosmochimica Acta*, 70:931–946.
<https://doi.org/10.1016/j.gca.2005.10.023>
- Kohn, M.J., Schoeninger, M.J., and Valley, J.W. 1996. Herbivore tooth oxygen isotope compositions: Effects of diet and physiology. *Geochimica et Cosmochimica Acta*, 60:3889–3896.
[https://doi.org/10.1016/0016-7037\(96\)00248-7](https://doi.org/10.1016/0016-7037(96)00248-7)
- Kohn, M.J., Schoeninger, M.J., and Valley, J.W. 1998. Variability in oxygen isotope compositions of herbivore teeth: reflections of seasonality or developmental physiology. *Chemical Geology*, 152:97–112.
[https://doi.org/10.1016/S0009-2541\(98\)00099-0](https://doi.org/10.1016/S0009-2541(98)00099-0)
- Krigbaum, J., Berger, M.H., Daegling, D.J., and McGraw, W.S. 2013. Stable isotope canopy effects for sympatric monkeys at Taï Forest, Côte d'Ivoire. *Biology Letters*, 9:20130466.
<https://doi.org/10.1098/rsbl.2013.0466>
- Lazagabaster, I.A., Cerling, T.E., and Faith, J.T. 2021. A Late Pleistocene third molar of *Hylochoerus* (Suidae, Mammalia) from Rusinga Island, Kenya: paleoenvironmental implications and a note on the hypsodonty of African forest hogs. *Historical Biology*, 33:3673–3685.
<https://doi.org/10.1080/08912963.2021.1887861>
- Leakey, M. 1985. Early Miocene cercopithecids from Buluk, northern Kenya. *Folia Primatologica*, 44:1–14.
<https://doi.org/10.1159/000156194>

- Leakey, M. and Walker, A. 1997. *Afropithecus*, p. 225–239. In Begun, D.R., Ward, C.V., and Rose, M.D. (eds.), Function, Phylogeny, and Fossils. Advances in Primatology. Springer, Boston, MA.
https://doi.org/10.1007/978-1-4899-0075-3_11
- Leakey, M., Grossman, A., Gutierrez, M., and Fleagle, J.G. 2011. Faunal change in the Turkana Basin during the Late Oligocene and Miocene. *Evolutionary Anthropology*, 20:238–253.
- Leakey, R.E.F. and Walker, A. 1985. New higher primates from the early Miocene of Buluk, Kenya. *Nature*, 318:173–175.
<https://doi.org/10.1038/318173a0>
- Lee-Thorp, J.A. and van der Merwe, N.J. 1991. Aspects of the chemistry of modern and fossil biological apatites. *Journal of Archaeological Science*, 18:343–354.
[https://doi.org/10.1016/0305-4403\(91\)90070-6](https://doi.org/10.1016/0305-4403(91)90070-6)
- Lee-Thorp, J.A., Sealy, J.C., and van der Merwe, N.J. 1989. Stable carbon isotope ratio differences between bone collagen and bone apatite, and their relationship to diet. *Journal of Archaeological Science*, 16:585–599.
[https://doi.org/10.1016/0305-4403\(89\)90024-1](https://doi.org/10.1016/0305-4403(89)90024-1)
- Levin, N.E., Quade, J., Simpson, S.W., Semaw, S., and Rogers, M. 2004. Isotopic evidence for Plio-Pleistocene environmental change at Gona, Ethiopia. *Earth and Planetary Science Letters*, 219:93–110.
[https://doi.org/10.1016/S0012-821X\(03\)00707-6](https://doi.org/10.1016/S0012-821X(03)00707-6)
- Levin, N.E., Cerling, T.E., Passey, B.H., Harris, J.M., and Ehleringer, J.R. 2006. A stable isotope aridity index for terrestrial environments. *Proceedings of the National Academy of Sciences of the United States of America*, 103:11201–11205.
<https://doi.org/10.1073/pnas.0604719103>
- Levin, N.E., Simpson, S.W., Quade, J., Cerling, T.E., and Frost, S.R. 2008. Herbivore enamel carbon isotopic composition and the environmental context of *Ardipithecus* at Gona, Ethiopia. In Quade, J. and Wynn, J.G. (eds.), The Geology of Early Humans in the Horn of Africa (Geological Society of America), 446:215–234.
[https://doi.org/10.1130/2008.2446\(10\)](https://doi.org/10.1130/2008.2446(10))
- Linder, H.P. 2017. East African Cenozoic vegetation history. *Evolutionary Anthropology: Issues, News, and Reviews*, 26:300–312.
<https://doi.org/10.1002/evan.21570>
- Liu, A.G.S.C., Seiffert, E.R., and Simons, E.L. 2008. Stable isotope evidence for an amphibious phase in early proboscidean evolution. *Proceedings of the National Academy of Sciences*, 105:5786–5791.
<https://doi.org/10.1073/pnas.0800884105>
- Liutkus-Pierce, C.M., Takashita-Bynum, K.K., Beane, L.A., Edwards, C.T., Burns, O.E., Mana, S., Hemming, S., Grossman, A., Wright, J.D., and Kirera, F.M. 2019. Reconstruction of the Early Miocene Critical Zone at Loperot, Southwestern Turkana, Kenya. *Frontiers in Ecology and Evolution*, 7:44.
<https://doi.org/10.3389/fevo.2019.00044>
- Locke, E.M., Benefit, B.R., Kimock, C.M., Miller, E.R., and Nengo, I. 2020. New dentognathic fossils of *Noropithecus bulukensis* (Primates, Victoriapithecidae) from the late Early Miocene of Buluk, Kenya. *Journal of Human Evolution*, 148:102886.
<https://doi.org/10.1016/j.jhevol.2020.102886>
- Lukens, W.E., Lehmann, T., Peppe, D.J., Fox, D.L., Driese, S.G., and McNulty, K.P. 2017a. The Early Miocene Critical Zone at Karungu, Western Kenya: an equatorial, open habitat with few primate remains. *Frontiers in Earth Science*, 5:87.
<https://doi.org/10.3389/feart.2017.00087>
- Lukens, W.E., Peppe, D.J., Locke, E., Miller, E., Deino, A.L., and Oginga, K.O. 2017b. Paleoenvironments and mammalian fauna of the early Miocene fossil site at Buluk, Kenya. *American Journal of Physical Anthropology*, 162(S64):268–269.
- Lukens, W., Peppe, D., Deino, A.L., Fox, D.L., Beverly, E., and Miller, E. 2021. A woodland-savanna mosaic in the early middle Miocene at Buluk, Turkana Basin, Kenya. *Geological Society of America Abstracts with Programs*, 53:6.
<https://doi.org/10.1130/abs/2021AM-363879>

- Luyt, J., Hare, V.J., and Sealy, J. 2019. The relationship of ungulate $\delta^{13}\text{C}$ and environment in the temperate biome of southern Africa, and its palaeoclimatic application. *Palaeogeography, Palaeoclimatology, Palaeoecology*, 514:282–291.
<https://doi.org/10.1016/j.palaeo.2018.10.016>
- MacLatchy, L.M., Cote, S.M., Deino, A.L., Kityo, R.M., Mugume, A.A., Rossie, J.B., Sanders, W.J., Cosman, M.N., Driese, S.G., Fox, D.L., Freeman, A.J., Jansma, R.J.W., Jenkins, K.E.H., Kinyanjui, R.N., Lukens, W.E., McNulty, K.P., Novello, A., Peppe, D.J., Strömberg, C.A.E., Uno, K.T., Winkler, A.J., and Kingston, J.D. 2023. The evolution of hominoid locomotor versatility: evidence from Moroto, a 21 Ma site in Uganda. *Science*, 380:eabq2835.
<https://doi.org/10.1126/science.abq2835>
- Malone, M.A., MacLatchy, L.M., Mitani, J.C., Kityo, R., and Kingston, J.D. 2021. A chimpanzee enamel-diet $\delta^{13}\text{C}$ enrichment factor and a refined enamel sampling strategy: Implications for dietary reconstructions. *Journal of Human Evolution*, 159:103062.
<https://doi.org/10.1016/J.JHEVOL.2021.103062>
- Martin, J.E., Vance, D., and Balter, V. 2015. Magnesium stable isotope ecology using mammal tooth enamel. *Proceedings of the National Academy of Sciences*, 112:430–435.
<https://doi.org/10.1073/pnas.1417792112>
- Mayr, A. and Mayr, G. 2014. A hoatzin fossil from the middle Miocene of Kenya documents the past occurrence of modern-type Opisthocomiformes in Africa. *The Auk: Ornithological Advances*, 131:55–60.
<https://doi.org/10.1642/AUK-13-134.1>
- Mayr, G. 2014. On the Middle Miocene avifauna of Maboko Island, Kenya. *Geobios*, 47:133–146.
<https://doi.org/10.1016/j.geobios.2014.03.001>
- McDougall, I. and Watkins, R.T. 1985. Age of hominoid-bearing sequence at Buluk, northern Kenya. *Nature*, 318:175–178.
<https://doi.org/10.1038/318175a0>
- Michel, L.A., Peppe, D.J., Lutz, J.A., Driese, S.G., Dunsworth, H.M., Harcourt-Smith, W.E.H., Horner, W.H., Lehmann, T., Nightingale, S., and McNulty, K.P. 2014. Remnants of an ancient forest provide ecological context for Early Miocene fossil apes. *Nature Communications*, 5:611–614.
<https://doi.org/10.1038/ncomms4236>
- Michel, L.A., Lehmann, T., McNulty, K.P., Driese, S.G., Dunsworth, H., Fox, D.L., Harcourt-Smith, W.E.H., Jenkins, K., and Peppe, D.J. 2020. Sedimentological and palaeoenvironmental study from Waregi Hill in the Hiwegi Formation (early Miocene) on Rusinga Island, Lake Victoria, Kenya. *Sedimentology*, 67:3567–3594.
<https://doi.org/10.1111/sed.12762>
- Miller, E.R., Benefit, B.R., McCrossin, M.L., Plavcan, J.M., Leakey, M.G., El-Barkooky, A.N., Hamdan, M.A., Abdel Gawad, M.K., Hassan, S.M., and Simons, E.L. 2009. Systematics of early and middle Miocene Old World monkeys. *Journal of Human Evolution*, 57:195–211.
<https://doi.org/10.1016/j.jhevol.2009.06.006>
- Miller, E.R., Gunnell, G.F., Gawad, M.A., Hamdan, M., El-Barkooky, A.N., Clementz, M.T., and Hassan, S.M. 2014. Anthracotheres from Wadi Moghra, Early Miocene, Egypt. *Journal of Paleontology*, 88: 967–981.
<https://doi.org/10.1666/13-122>
- Morgan, M.E., Kingston, J.D., and Marino, B.D. 1994. Carbon isotopic evidence for the emergence of C4 plants in the Neogene from Pakistan and Kenya. *Nature*, 367:162–165.
<https://doi.org/10.1038/367162a0>
- Morlo, M., Frisia, A., Miller, E., Locke, E., and Nengo, I. 2021. Systematics and paleobiology of Carnivora and Hyenaodontata from Buluk, Early Miocene, Kenya. *Acta Palaeontologica Polonica*, 66: 465–484.
<https://doi.org/10.4202/app.00794.2020>
- Munday, C., Savage, N., Jones, R.G., and Washington, R. 2023. Valley formation aridifies East Africa and elevates Congo Basin rainfall. *Nature*, 615: 276–279.
<https://doi.org/10.1038/s41586-022-05662-5>
- Napier, J.R. 1967. Evolutionary aspects of primate locomotion. *American Journal of Physical Anthropology*, 27:333–341.
<https://doi.org/10.1002/ajpa.1330270306>

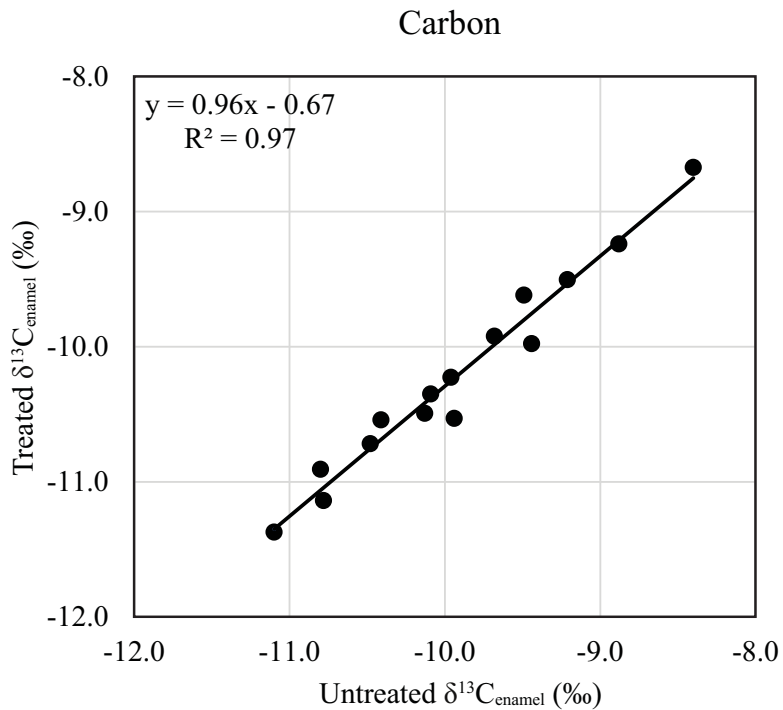
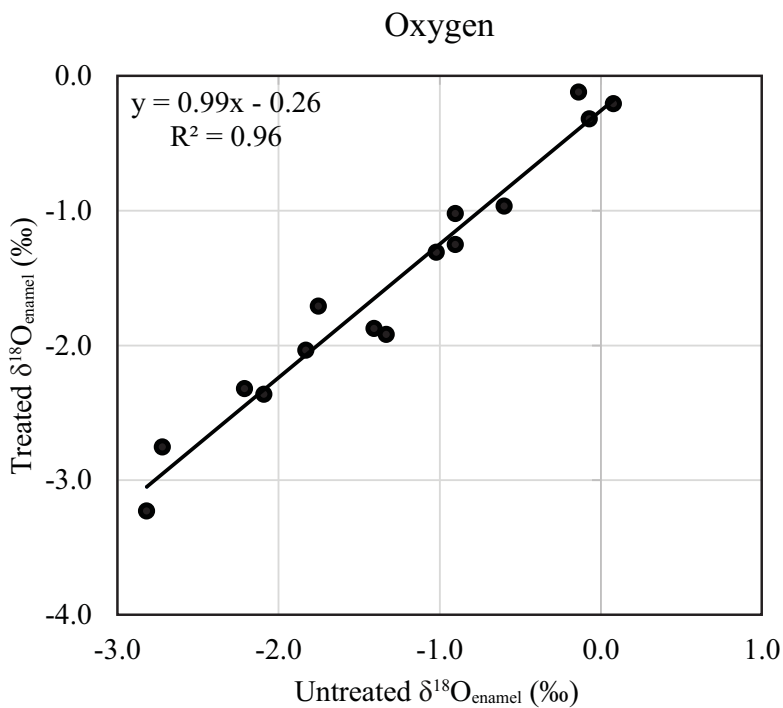
- Nelson, S.V. 2007. Isotopic reconstructions of habitat change surrounding the extinction of *Sivapithecus*, a Miocene hominoid, in the Siwalik Group of Pakistan. *Palaeogeography, Palaeoclimatology, Palaeoecology*, 243:204–222.
<https://doi.org/10.1016/j.palaeo.2006.07.017>
- Nelson, S.V. 2013. Chimpanzee fauna isotopes provide new interpretations of fossil ape and hominin ecologies. *Proceedings of the Royal Society B: Biological Sciences*, 280:20132324.
<https://doi.org/10.1098/rspb.2013.2324>
- Nesbit Evans, E.M., Wildlife, V., Van Couvering, J.A.H., and Andrews, P. 1981. Palaeoecology of Miocene Sites in Western Kenya. *Journal of Human Evolution*, 10:99–116.
- Nishimura, A.C., Russo, G.A., Nengo, I.O., and Miller, E.R. 2022. Morphological affinities of a fossil ulna (KNM-WS 65401) from Buluk, Kenya. *Journal of Human Evolution*, 166:103177.
<https://doi.org/10.1016/j.jhevol.2022.103177>
- Paquette, J. and Drapeau, M.S.M. 2021. Environmental comparisons of the Awash Valley, Turkana Basin and lower Omo Valley from upper Miocene to Holocene as assessed from stable carbon and oxygen isotopes of mammalian enamel. *Palaeogeography, Palaeoclimatology, Palaeoecology*, 562:110099.
<https://doi.org/10.1016/j.palaeo.2020.110099>
- Passey B.H., Robinson, T.F., Ayliffe, L.K., Cerling, T.E., Sponheimer, M., Dearing, M.D., Roeder, B.L., and Ehleringer, J.R. 2005. Carbon isotope fractionation between diet, breath CO₂, and bioapatite in different mammals. *Journal of Archaeological Science*, 32:1459–1470.
<https://doi.org/10.1016/j.jas.2005.03.015>
- Peppe, D., Cote, S.M., Deino, A.L., Fox, D.L., Kingston, J.D., Kinyanjui, R.N., Lukens, W.E., MacLatchy, L.M., Novello, A., Strömberg, C.A.E., Driese, S.G., Garrett, N.D., Hillis, K.R., Jacobs, B.F., Jenkins, K.E.H., Kityo, R.M., Lehmann, T., Manthi, F.K., Mbua, E.N., Michel, L.A., Miller, E.R., Mugume, A.A.T., Muteti, S.N., Nengo, I.O., Oginga, K.O., Phelps, S.R., Polissar, P., Rossie, J.B., Stevens, N.J., Uno, K.T., and McNulty, K.P. 2023. Oldest evidence of abundant C₄ grasses and habitat heterogeneity in eastern Africa. *Science*, 380:173–177.
<https://doi.org/10.1126/science.abq2834>
- Pickford, M. 1981. Preliminary Miocene mammalian biostratigraphy for Western Kenya. *Journal of Human Evolution*, 10:73–97.
[https://doi.org/10.1016/S0047-2484\(81\)80026-7](https://doi.org/10.1016/S0047-2484(81)80026-7)
- Pickford, M. 1983a. Sequence and environments of the Lower and Middle Miocene hominoids of Western Kenya, p. 421–439. In Ciochon, R.L. and Corruccini, R.D. (eds.), *New Interpretations of Ape and Human Ancestry*. Plenum Press, New York.
https://doi.org/10.1007/978-1-4684-8854-8_16
- Pickford, M. 1983b. On the origins of Hippopotamidae together with descriptions of two new species, a new genus and a new subfamily from the Miocene of Kenya. *Geobios*, 16:193–217.
[https://doi.org/10.1016/S0016-6995\(83\)80019-9](https://doi.org/10.1016/S0016-6995(83)80019-9)
- Pickford, M. 1995. Fossil land snails of East Africa and their palaeoecological significance. *Journal of African Earth Sciences*, 20:167–226.
[https://doi.org/10.1016/0899-5362\(95\)94397-R](https://doi.org/10.1016/0899-5362(95)94397-R)
- Pickford, M., Sawada, Y., Tayama, R., Matsuda, Y., Itaya, T., Hyodo, H., and Senut, B. 2006. Refinement of the age of the Middle Miocene Fort Ternan Beds, Western Kenya, and its implications for Old World biochronology. *Comptes Rendus Geoscience*, 338:545–555.
<https://doi.org/10.1016/J.CRTE.2006.02.010>
- Polissar, P.J., Rose, C., Uno, K.T., Phelps, S.R., and deMenocal, P. 2019. Synchronous rise of African C₄ ecosystems 10 million years ago in the absence of aridification. *Nature Geoscience*, 12:657–660.
<https://doi.org/10.1038/s41561-019-0399-2>
- R Core Team 2021. R: A language and environment for statistical computing. R Foundation for Statistical Computing, Vienna, Austria.
- Retallack, G.J. 1992. Middle Miocene fossil plants from Fort Ternan (Kenya) and evolution of African grasslands. *Paleobiology*, 18:383–400.
<https://doi.org/10.1017/S0094837300010964>
- Retallack, G.J., Dugas, D.P., and Bestland, E.A. 1990. Fossil soils and grasses of a middle Miocene East African Grassland. *Science*, 247:1325–1328.
<https://doi.org/10.1126/science.247.4948.1325>

- Retallack, G.J., Wynn, J.G., Benefit, B.R., and Mccrossin, M.L. 2002. Paleosols and paleoenvironments of the middle Miocene, Maboko Formation, Kenya. *Journal of Human Evolution*, 42:659–703.
<https://doi.org/10.1006/JHEV.2002.0553>
- Roberts, P., Blumenthal, S.A., Dittus, W., Wedage, O., and Lee-Thorp, J.A. 2017. Stable carbon, oxygen, and nitrogen, isotope analysis of plants from a South Asian tropical forest: Implications for primatology. *American Journal of Primatology*, 79:e22656.
<https://doi.org/10.1002/ajp.22656>
- Robinson, J.R., Rowan, J., Barr, W.A., and Sponheimer, M. 2021. Intrataxonomic trends in herbivore enamel $\delta^{13}\text{C}$ are decoupled from ecosystem woody cover. *Nature Ecology & Evolution*, 5:995–1002.
<https://doi.org/10.1038/s41559-021-01455-7>
- Rose, M.D., Leakey, M.G., Leakey, R.E.F., and Walker, A.C. 1992. Postcranial specimens of *Simiolus enjessi* and other primitive catarrhines from the early Miocene of Lake Turkana, Kenya. *Journal of Human Evolution*, 22:171–237.
[https://doi.org/10.1016/S0047-2484\(05\)80006-5](https://doi.org/10.1016/S0047-2484(05)80006-5)
- Rowan, J., Adrian, B., and Grossman, A. 2015. The first skull of *Sivameryx africanus* (Anthracotheriidae, Bothriodontinae) from the early Miocene of East Africa. *Journal of Vertebrate Paleontology*, 35:e928305.
<https://doi.org/10.1080/02724634.2014.928305>
- Rozanski, K., Araguas-Araguas, L., and Gonfiantini, R. 1993. Isotopic patterns in modern global precipitation, p. 1–36. In Swart, P.K., Lohmann, K.C., McKenzie, J., and Savin, S. (eds.), *Climate Change in Continental Isotopic Records*, Volume 78. The American Geophysical Union, Washington, DC.
<https://doi.org/10.1029/GM078p0001>
- Saarinen, J. and Lister, A.M. 2023. Fluctuating climate and dietary innovation drove ratcheted evolution of proboscidean dental traits. *Nature Ecology & Evolution*, 7:1490–1502.
<https://doi.org/10.1038/s41559-023-02151-4>
- Schoeninger, M.J., Reeser, H., and Hallin, K. 2003. Paleoenvironment of *Australopithecus anamensis* at Allia Bay, East Turkana, Kenya: evidence from mammalian herbivore enamel stable isotopes. *Journal of Anthropological Archaeology*, 22:200–207.
[https://doi.org/10.1016/S0278-4165\(03\)00034-5](https://doi.org/10.1016/S0278-4165(03)00034-5)
- Sepulchre, P., Ramstein, G., Fluteau, F., Schuster, M., Tiercelin, J.J., and Brunet, M. 2006. Tectonic uplift and Eastern Africa aridification. *Science*, 313:1419–1423.
<https://doi.org/10.1126/science.1129158>
- Shipman, P. 1986. Paleoecology of Fort Ternan reconsidered. *Journal of Human Evolution*, 15:193–204.
[https://doi.org/10.1016/S0047-2484\(86\)80045-8](https://doi.org/10.1016/S0047-2484(86)80045-8)
- Shipman, P., Walker, A., Van Couvering, J.A., Hooker, P.J., and Miller, J.A. 1981. The Fort Ternan hominoid site, Kenya: Geology, age, taphonomy and paleoecology. *Journal of Human Evolution*, 10:49–72.
[https://doi.org/10.1016/S0047-2484\(81\)80025-5](https://doi.org/10.1016/S0047-2484(81)80025-5)
- Spinage, C.A. 1976. Age determination of the female Grant's gazelle. *African Journal of Ecology*, 14:121–134.
<https://doi.org/10.1111/j.1365-2028.1976.tb00157.x>
- Sponheimer, M. and Lee-Thorp, J.A. 1999. Oxygen isotopes in enamel carbonate and their ecological significance. *Journal of Archaeological Science*, 26:723–728.
<https://doi.org/10.1006/JASC.1998.0388>
- Sponheimer, M., Lee-Thorp, J.A., DeRuiter, D.J., Smith, J.M., van der Merwe, N.J., Reed, K., Grant, C.C., Ayliffe, L.K., Robinson, T.F., Heidelberger, C., and Marcus, W. 2003. Diets of Southern African Bovidae: stable isotope evidence. *Journal of Mammalogy*, 84:471–479.
[https://doi.org/10.1644/1545-1542\(2003\)084<0471:DOSABS>2.0.CO;2](https://doi.org/10.1644/1545-1542(2003)084<0471:DOSABS>2.0.CO;2)
- Sternberg, L.S.L., Mulkey, S.S., and Wright, S.J. 1989. Oxygen isotope ratio stratification in a tropical moist forest. *Oecologia*, 81:51–56.
<https://doi.org/10.1007/BF00377009>
- Tejada-Lara, J.V., MacFadden, B.J., Bermudez, L., Rojas, G., Salas-Gismondi, R., and Flynn, J.J. 2018. Body mass predicts isotope enrichment in herbivorous mammals. *Proceedings of the Royal Society B*, 285:20181020.
<https://doi.org/10.1098/RSPB.2018.1020>

- Temerin, L. and Cant, J. 1983. The evolutionary divergence of Old World monkeys and apes. *American Naturalist*, 122:335–351.
<https://doi.org/10.1086/284139>
- Tieszen, L.L., Senyimba, M.M., Imbamba, S.K., and Troughton, J.H. 1979. The distribution of C₃ and C₄ grasses and carbon isotope discrimination along an altitudinal and moisture gradient in Kenya. *Oecologia*, 37:337–350.
<https://doi.org/10.1007/BF00347910>
- Tipple, B.J., Meyers, S.R., and Pagani, M. 2010. Carbon isotope ratio of Cenozoic CO₂: A comparative evaluation of available geochemical proxies. *Paleoceanography*, 25:1–11.
<https://doi.org/10.1029/2009PA001851>
- Tütken, T. and Absolon, J. 2015. Late Oligocene ambient temperatures reconstructed by stable isotope analysis of terrestrial and aquatic vertebrate fossils of Enspel, Germany. *Palaeobiodiversity and Palaeoenvironments*, 95:17–31.
<https://doi.org/10.1007/s12549-014-0183-7>
- Uno, K.T., Cerling, T.E., Harris, J.M., Kunitatsu, Y., Leakey, M.G., Nakatsukasa, M., and Nakaya, H. 2011. Late Miocene to Pliocene carbon isotope record of differential diet change among East African herbivores. *Proceedings of the National Academy of Sciences*, 108:6509–6514.
<https://doi.org/10.1073/pnas.1018435108>
- Uno, K.T., Polissar, P.J., Jackson, K.E., and deMenocal, P.B. 2016. Neogene biomarker record of vegetation change in eastern Africa. *Proceedings of the National Academy of Sciences*, 113:6355–6363.
<https://doi.org/10.1073/pnas.1521267113>
- Uno, K.T., Rivals, F., Bibi, F., Pante, M., and Njau, J. 2018. Large mammal diets and paleoecology across the Oldowan–Acheulean transition at Olduvai Gorge, Tanzania from stable isotope and tooth wear analyses. *Journal of Human Evolution*, 120:76–91.
<https://doi.org/10.1016/J.JHEVOL.2018.01.002>
- van der Made, J. 1996. Listriodontinae (Suidae, Mammalia), their evolution, systematics and distribution in time and space. *Mededelingen van de Werkgroep voor Tertiaire en Kwartaire Geologie*, 33:3–254.
- van der Merwe, N.J. and Medina, E. 1989. Photosynthesis and ¹³C/¹²C ratios in Amazonian rain forests. *Geochimica et Cosmochimica Acta*, 53:1091–1094.
[https://doi.org/10.1016/0016-7037\(89\)90213-5](https://doi.org/10.1016/0016-7037(89)90213-5)
- van der Merwe, N.J. and Medina, E. 1991. The canopy effect, carbon isotope ratios and foodwebs in Amazonia. *Journal of Archaeological Science*, 18:249–259.
[https://doi.org/10.1016/0305-4403\(91\)90064-V](https://doi.org/10.1016/0305-4403(91)90064-V)
- Vogel, J.C. 1978. Recycling of carbon in a forest environment. *Oecologia Plantarum*, 13:89–94.
- Watkins, R.T. 1989. The Buluk Member, a fossil hominoid-bearing sedimentary sequence of Miocene age from northern Kenya. *Journal of African Earth Sciences (and the Middle East)*, 8:107–112.
[https://doi.org/10.1016/S0899-5362\(89\)80015-6](https://doi.org/10.1016/S0899-5362(89)80015-6)
- Wheeler, E.A., Wiemann, M.C., and Fleagle, J.G. 2007. Woods from the Miocene Bakate Formation, Ethiopia Anatomical characteristics, estimates of original specific gravity and ecological inferences. *Review of Palaeobotany and Palynology*, 146:193–207.
<https://doi.org/10.1016/j.revpalbo.2007.04.002>
- Wichura, H., Jacobs, L.L., Lin, A., and Clemens, M. 2015. A 17-My-old whale constrains onset of uplift and climate change in East Africa. *Proceedings of the National Academy of Sciences*, 112:3910–3915.
<https://doi.org/10.1073/pnas.1421502112>
- Young, H.J. and Young, T.P. 1983. Local distribution of C₃ and C₄ grasses in sites of overlap on Mount Kenya. *Oecologia*, 58:373–377.
<https://doi.org/10.1007/BF00385238>

APPENDIX 1.

Bivariate plots of $\delta^{13}\text{C}_{\text{enamel}}$ (A) and $\delta^{18}\text{O}_{\text{enamel}}$ values (B) of treated versus untreated enamel samples. $\delta^{13}\text{C}$ values are in parts per million (\textperthousand) units. Linear regression lines and equations are reported on plots.

A**B**

APPENDIX 2.

Carbon and oxygen data of fossil herbivore enamel from Buluk.

Accession no.	Taxon	$\delta^{13}\text{C}_{\text{enamel}}$				$\delta^{18}\text{O}_{\text{enamel}}$			
		$\delta^{13}\text{C}$ untreated	$\delta^{13}\text{C}$ treated	Untreated v. treated difference	$\delta^{13}\text{C}_{1750}$ 17.2ma	$\delta^{13}\text{C}_{1750}$ 16ma ¹	$\delta^{18}\text{O}$ untreated	$\delta^{18}\text{O}$ treated	
Cetartiodactyla									
Anthracotheriidae									
WS 12581	cf. <i>Sivameryx</i>	-9.4	-9.7		-9.9	-10.9	-4.4	-4.6	
WS 31258	cf. <i>Sivameryx</i>	-9.7	-10		-10.3	-11.3	-5	-5.2	
B 480	cf. <i>Sivameryx</i>	-10.1	-10.3		-10.6	-11.4	-2.9	-3.1	
WS 12841	cf. <i>Sivameryx</i>	-8.5	-8.9		-9	-10.1	2.2	2	
Suidae									
B 152	<i>Megalochoerus marymuunguae</i>	-10.5	-10.7		-11	-12	0.8	0.5	
B 235	<i>Megalochoerus marymuunguae</i>	-10.5	-10.8		-11.1	-12	0	-0.3	
WS 12590	<i>Megalochoerus marymuunguae</i>	-10.3	-10.6		-10.8	-11.8	1.7	1.4	
WS 12594	<i>Megalochoerus marymuunguae</i>	-9.6	-9.9		-10.1	-11.1	0.8	0.5	
WS 12656	<i>Megalochoerus marymuunguae</i>	-10.4	-10.7		-10.9	-11.9	-0.8	-1	
Sanitheriidae									
WS 12591	<i>Diamantohyus africanus</i>	-8.8	-9.1		-9.3	-10.4	-2	-2.2	
WS 12592	<i>Diamantohyus africanus</i>	-9.9	-10.1		-10.4	-11.4	-2.6	-2.8	
WS 12593	<i>Diamantohyus africanus</i>	-8.5	-8.9		-9	-10.1	-2.5	-2.7	
Tragulidae									
B 406	<i>Dorcatherium pigotti</i>	-8.9	-9.2		-9.4	-10.5	-4	-4.2	
WS 12803	<i>Dorcatherium pigotti</i>	-9.1	-9.4		-9.6	-10.6	-4.3	-4.5	
WS 12819	<i>Dorcatherium pigotti</i>	-9	-9.3		-9.5	-10.6	0	-0.3	
WS 49492	<i>Dorcatherium pigotti</i>	-9.6	-9.9		-10.2	-11.2	-1.9	-2.1	
WS 49508*	<i>Dorcatherium pigotti</i>	-9.7	-9.9	0.2	-10.2	-11.2	-2.7	-3	
Giraffidae									
B 066	<i>Canthumeryx sirtensis</i>	-8.5	-8.8		-9	-10.1	3	2.7	
B 082	<i>Canthumeryx sirtensis</i>	-9.5	-9.8		-10	-11.1	2.8	2.5	
B 487	<i>Canthumeryx sirtensis</i>	-10.7	-10.9		-11.2	-12.2	1.6	1.3	
WS 12840	<i>Canthumeryx sirtensis</i>	-9.3	-9.6		-9.8	-10.8	3.8	3.5	

Accession no.	Taxon	δ ¹³ C			δ ¹³ C _{enamel} Untreated v. treated difference		δ ¹⁸ O _{enamel} Untreated v. treated difference		
		untreated	δ ¹³ C treated	difference	17.2ma	16ma ¹	untreated	δ ¹⁸ O treated	difference
WS 49486	<i>Canthumeryx sirtensis</i>	-11.6	-11.8		-12.1	-13	-0.3	-0.6	
WS 49502	<i>Canthumeryx sirtensis</i>	-10.2	-10.4		-10.7	-11.7	2.2	1.9	
Perissodactyla									
Rhinocerotidae									
B 102	<i>Brachypotherium minor</i>	-10.4	-10.7		-10.9	-11.9	-1.4	-1.6	
B 266*	<i>Brachypotherium minor</i>	-10.1	-10.4	0.3	-10.6	-11.6	-0.1	-0.3	0.2
B 280	<i>Brachypotherium minor</i>	-10.2	-10.5		-10.8	-11.8	0.1	-0.1	
B 494	<i>Brachypotherium minor</i>	-10.6	-10.8		-11.1	-12.1	-2.2	-2.4	
WS 136	<i>Brachypotherium minor</i>	-11.5	-11.8		-12.1	-13	-3.4	-3.6	
WS 15	<i>Brachypotherium minor</i>	-10.3	-10.6		-10.8	-11.8	0.5	0.2	
WS 31253*	<i>Brachypotherium minor</i>	-10.8	-10.9	0.1	-11.3	-12.2	-0.9	-1.2	0.3
B 388	Rhinocerotidae sp.	-11.8	-12		-12.3	-13.3	-2.2	-2.5	
B 441	Rhinocerotidae sp.	-10	-10.3		-10.6	-11.6	-1	-1.3	
WS 12843	Rhinocerotidae sp.	-10	-10.3		-10.6	-11.6	-0.4	-0.6	
Hyracoidea									
Titanohyracidae									
WS 12795	<i>Afrohyrax championi</i>	-10.1	-10.4		-10.6	-11.6	0.2	-0.1	
WS 22	<i>Afrohyrax championi</i>	-10	-10.3		-10.5	-11.5	1.9	1.6	
Proboscidea									
Deinotheriidae									
B 273*	<i>Prodeinotherium hobleyi</i>	-9.9	-10.5	0.6	-10.5	-11.8	0.1	-0.2	0.1
B 380	<i>Prodeinotherium hobleyi</i>	-9.9	-10.2		-10.4	-11.4	-1.6	-1.8	
B052*	<i>Prodeinotherium hobleyi</i>	-10.8	-11.1	0.3	-11.3	-12.4	-0.6	-0.9	0.3
WS 12665*	<i>Prodeinotherium hobleyi</i>	-10.5	-10.7	0.2	-11	-12	-2.2	-2.4	0.2
WS 128D*	<i>Prodeinotherium hobleyi</i>	-11.1	-11.4	0.3	-11.6	-12.6	-0.9	-1.2	0.3
WS 131	<i>Prodeinotherium hobleyi</i>	-10.8	-11		-11.3	-12.3	-1.8	-2.1	
WS 17	<i>Prodeinotherium hobleyi</i>	-9.1	-9.4		-9.6	-10.6	-5.8	-6	

Accession no.	Taxon	$\delta^{13}\text{C}_{\text{enamel}}$			$\delta^{18}\text{O}_{\text{enamel}}$			$\delta^{18}\text{O}_{\text{enamel}}$		
		$\delta^{13}\text{C}$ untreated	$\delta^{13}\text{C}$ treated	Untreated v. treated difference	$\delta^{13}\text{C}_{1750}$ 17.2ma	$\delta^{13}\text{C}_{1750}$ 16ma ¹	$\delta^{18}\text{O}$ untreated	$\delta^{18}\text{O}$ treated	Untreated v. treated difference	
WS 30725	<i>Prodeinotherium hobleyi</i>	-10.3	-10.6		-10.8	-11.8	-0.4	-0.6		
WS 30727	<i>Prodeinotherium hobleyi</i>	-11.3	-11.5		-11.8	-12.7	-6.2	-6.4		
WS 30728	<i>Prodeinotherium hobleyi</i>	-8.9	-9.3		-9.5	-10.5	-5.1	-5.3		
WS 4	<i>Prodeinotherium hobleyi</i>	-10.6	-10.9		-11.1	-12.1	-3.6	-3.8		
WS 45*	<i>Prodeinotherium hobleyi</i>	-10.1	-10.5	0.4	-10.7	-11.7	-2.8	-3	0.2	
WS 46	<i>Prodeinotherium hobleyi</i>	-9.9	-10.2		-10.4	-11.4	-0.2	-0.5		
WS 47	<i>Prodeinotherium hobleyi</i>	-9.7	-10		-10.3	-11.3	-6	-6.2		
WS 50	<i>Prodeinotherium hobleyi</i>	-9.4	-10		-10	-11.2	-1.8	-2		
WS 52	<i>Prodeinotherium hobleyi</i>	-9.4	-9.7		-9.9	-10.9	-4.2	-4.5		
WS 57	<i>Prodeinotherium hobleyi</i>	-9.5	-9.6		-10	-10.9	-1.4	-1.7		
WS 58	<i>Prodeinotherium hobleyi</i>	-10.6	-10.9		-11.1	-12.1	-3.6	-3.8		
WS 63	<i>Prodeinotherium hobleyi</i>	-10.3	-10.6		-10.9	-11.9	-3.3	-3.5		
Mammutidae										
B 359	<i>Zygolophodon</i> nov. sp.	-8.7	-9		-9.2	-10.2	-3	-3.2		
Gomphotheriidae										
B 271	<i>Archaeobelodon</i> sp. nov.	-8.9	-9.3		-9.5	-10.5	-2.6	-2.8		
B 325	<i>Archaeobelodon</i> sp. nov.	-9.3	-9.6		-9.9	-10.9	-2.3	-2.6		
B 002-2008*	<i>Protanancus</i> sp. nov.	-8.9	-9.2	0.3	-9.4	-10.5	-1	-1.3	0.3	
B 452*	<i>Afrochoerodon</i> <i>kisumuensis</i>	-8.4	-8.7	0.3	-8.9	-9.9	-1.8	-2.1	0.3	
Family indet										
B 244	Elephantimorph indet.	-8.7	-9.1		-9.3	-10.3	-3	-3.2		
B 267	Elephantimorph indet.	-8.9	-9.3		-9.5	-10.5	-4.2	-4.4		
B 268	Elephantimorph indet.	-8.5	-8.9		-9.1	-10.1	-4.9	-5.1		
WS 70*	Elephantimorph indet.	-9.2	-9.5	0.3	-9.7	-10.7	-2.1	-2.3	0.2	
WS 73	Elephantimorph indet.	-9	-9.3		-9.5	-10.5	-5.5	-5.7		
WS 74	Elephantimorph indet.	-9.2	-9.5		-9.7	-10.8	-6.2	-6.4		

Accession no.	Taxon	$\delta^{13}\text{C}_{\text{enamel}}$				$\delta^{18}\text{O}_{\text{enamel}}$		
		$\delta^{13}\text{C}$ untreated	$\delta^{13}\text{C}$ treated	v. treated difference	$\delta^{13}\text{C}_{1750}$ 17.2ma	$\delta^{13}\text{C}_{1750}$ 16ma ¹	$\delta^{18}\text{O}$ untreated	$\delta^{18}\text{O}$ treated
WS 77	Elephantimorph indet.	-8.5	-8.9		-9.1	-10.1	-4.8	-5
WS 88	Elephantimorph indet.	-9.2	-9.6		-9.8	-10.8	-4.9	-5.1
Mean difference between treated/ untreated				0.3				0.2

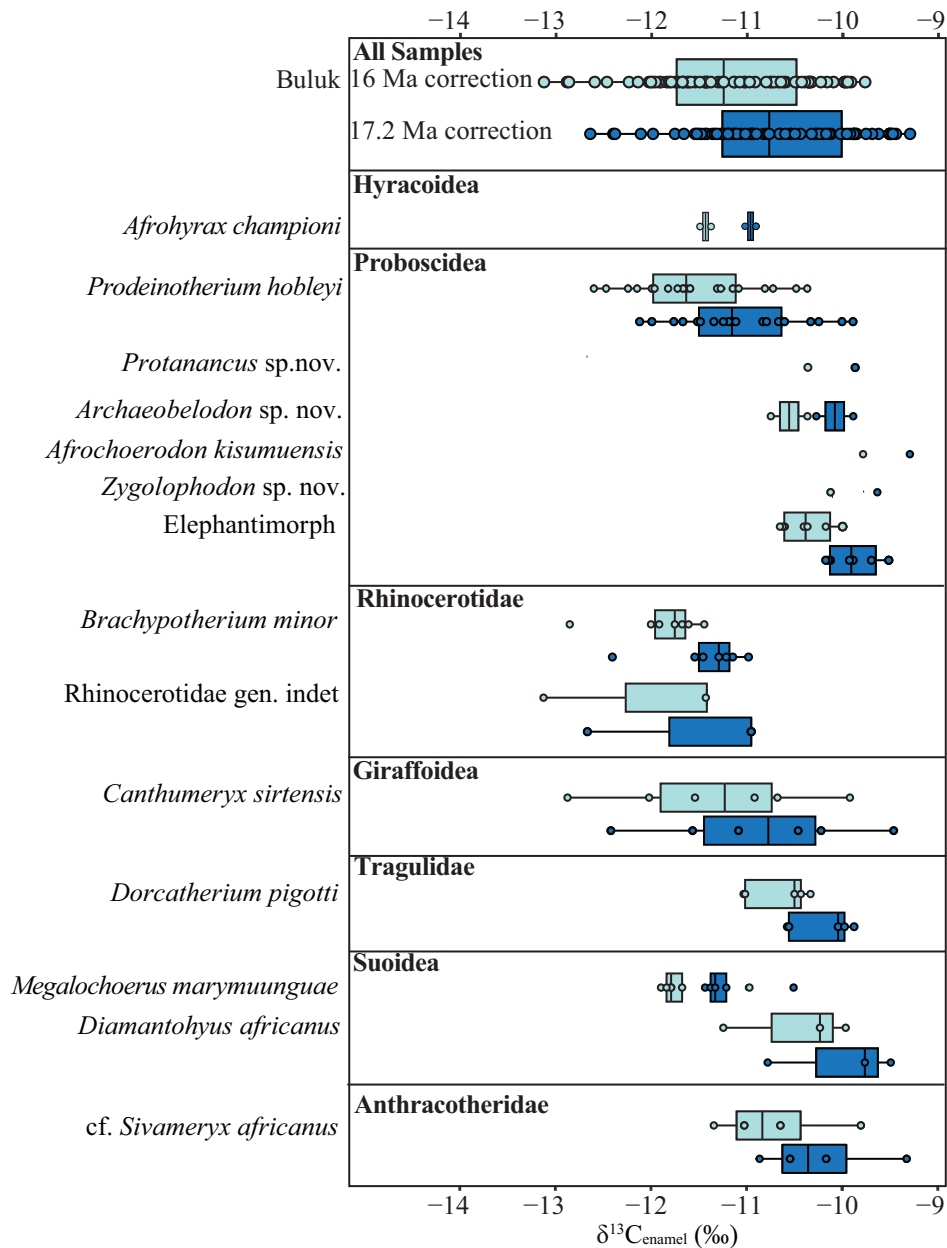
¹Using the high-resolution benthic estimates from Tipple et al., (2010), the mean $\delta^{13}\text{C}_{\text{atm}}$ value for an age of 15.9–16.3 Ma is -5.06‰. Therefore, -1.24‰ was added to treated $\delta^{13}\text{C}_{\text{enamel}}$ values for correction to $\delta^{13}\text{C}_{1750}$ values.

Columns labelled “ $\delta^{13}\text{C}_{\text{enamel}}$ Untreated” and “ $\delta^{18}\text{O}_{\text{enamel}}$ Untreated” refer to the carbon and oxygen isotopic values of untreated enamel, respectively. The columns labeled “ $\delta^{13}\text{C}_{\text{enamel}}$ Treated” and “ $\delta^{18}\text{O}_{\text{enamel}}$ Treated” refer to isotopic values after pretreatment and those generated for treatment using the regression equations in Appendix 1. Bolded and italicized values in this column indicate calculated treated $\delta^{13}\text{C}_{\text{enamel}}$ values. The columns labeled “ $\delta^{13}\text{C}_{\text{enamel}}$ Untreated v. treated difference” and “ $\delta^{18}\text{O}_{\text{enamel}}$ Untreated v. treated difference” refer to the absolute value of the difference between untreated and analyzed treated isotopic values. The column labeled “ $\delta^{13}\text{C}_{1750}$ _17.2ma” refers to the treated carbon isotopic values that have been corrected from to the reference $\delta^{13}\text{C}$ value of atmospheric CO_2 of 6.3‰ using at date of 17.2 Ma. The column labeled “ $\delta^{13}\text{C}_{1750}$ _16ma¹” refers to the treated carbon isotopic values that have been corrected from to the reference $\delta^{13}\text{C}$ value of atmospheric CO_2 of 6.3‰ using at date of 16 Ma.

*Indicates enamel samples for which both untreated and treated powder samples were isotopically analyzed using the procedure described in the Methods section of the main text.

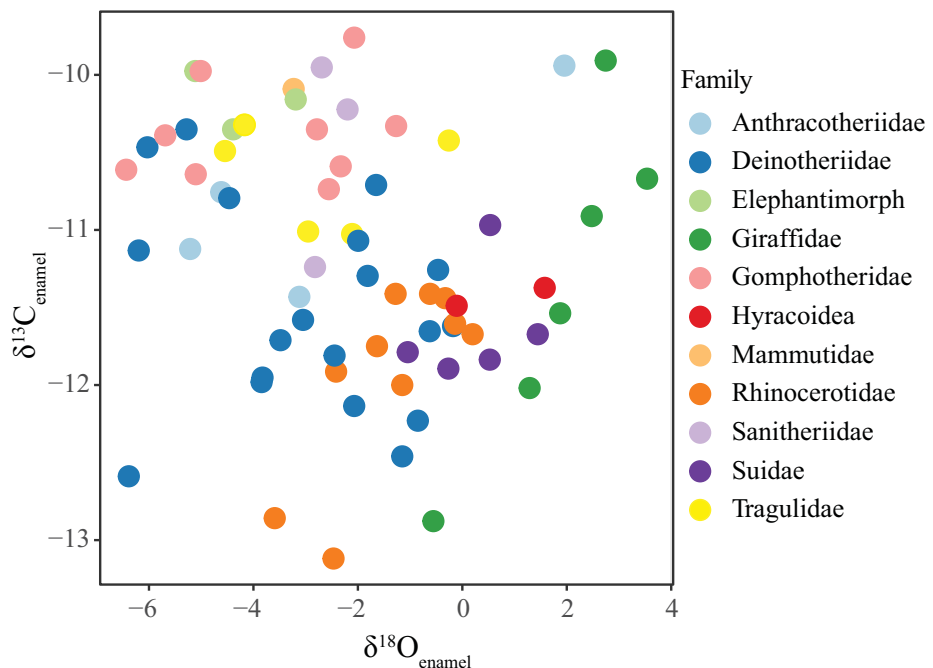
APPENDIX 3.

$\delta^{13}\text{C}_{\text{enamel}}$ value boxplots for Buluk, Maboko, and Fort Ternan displaying Buluk $\delta^{13}\text{C}_{1750}$ values corrected using a date of 17.2 Ma (light blue) and the terminal early Miocene date of 16 Ma (dark blue).



APPENDIX 4.

Bivariate plots of $\delta^{13}\text{C}$ versus $\delta^{18}\text{O}$ values for each taxonomic family sampled: Anthracotheriidae, Deinotheriidae, Gomphotheriidae, Mammutidae, Hyracoidea, Rhinocerotidae, Sanitheriidae, Suidae, Giraffidae, and Tragulidae. Gomphotheres, hyraxes, and rhinocerotids show no correlation or a slight positive correlation. Most mammalian families show a positive or no correlation between carbon and oxygen isotope values.



APPENDIX 5.

$\delta^{18}\text{O}_{\text{enamel}}$ value boxplots for Buluk, Moroto, Maboko, and Fort Ternan. Herbivore $\delta^{18}\text{O}_{\text{enamel}}$ values for Fort Ternan are from Cerling et al., (1997), $\delta^{18}\text{O}_{\text{enamel}}$ values for Maboko herbivores were taken from Arney et al. (2022), and $\delta^{18}\text{O}_{\text{enamel}}$ values for Moroto are extracted from MacLatchy et al., 2023. The top panel of $\delta^{18}\text{O}_{\text{enamel}}$ values labeled “All Samples” compares boxplots of all herbivore $\delta^{18}\text{O}_{\text{enamel}}$ values from each locality. Bottom panels compare $\delta^{18}\text{O}_{\text{enamel}}$ values of taxonomic families between sites.

